

Using the Epps effect to detect discrete processes

Patrick Chang^{a,b}, Etienne Pienaar^a, Tim Gebbie^a

^aDepartment of Statistical Science, University of Cape Town, Rondebosch 7700, South Africa

^bDepartment of Engineering Science, University of Oxford, Oxford OX1 3PJ, United Kingdom

Abstract

The Epps effect is key phenomenology relating to high frequency correlation dynamics in financial markets. We argue that it can be used to provide insight into whether tick data is best represented as samples from Brownian diffusions, or as samples from truly discrete events represented as connected point processes. We derive the Epps effect arising from asynchrony and provide a refined method to correct for the effect. We then propose three experiments which show how to discriminate between possible underlying representations. These in turn demonstrate how a simple Hawkes representation recovers phenomenology reported in the literature that cannot be recovered using a Brownian representation without additional *ad hoc* model complexity. However, complex *ad hoc* noise models built on Brownian motions cannot in general be discriminated relative to a Hawkes representation. Nevertheless, we argue that high frequency correlation dynamics are most faithfully recovered when tick data is represented as a web of interconnected discrete events rather than being samples from continuous Brownian diffusions even when combined with noise.

Keywords: Epps effect, Hawkes process, Asynchronous sampling

Contents

| | | |
|-------------------|---|-----------|
| 1 | Introduction | 1 |
| 2 | Asynchrony: Compensating for the Epps effect | 2 |
| 2.1 | The Epps effect from asynchrony | 2 |
| 2.2 | Correcting for asynchrony | 4 |
| 3 | Hawkes process | 5 |
| 4 | Simulation Experiments | 5 |
| 4.1 | Brownian price model | 6 |
| 4.2 | Market microstructure noise model | 7 |
| 4.3 | Hawkes price model | 8 |
| 5 | The residual Epps effect | 9 |
| 6 | Perspectives on noise and discreteness | 12 |
| 7 | Empirical Investigation | 13 |
| 8 | Conclusion | 15 |
| Appendix A | Estimators for market microstructure noise | 16 |

1. Introduction

Models are abstractions of reality which aim to faithfully recover, explain, and sometimes predict system observables. Ide-

ally, invoking *Occam's razor* and thus using the most parsimonious representation that fit the data. To interface such abstractions with real-world processes, models impose assumptions, whether they are clearly stated or implied. These assumptions govern how we treat certain empirical phenomenon. Here we are concerned with the decay of correlations as sampling intervals decrease in high frequency financial markets—the Epps effect (Epps, 1979). Models where the underlying representation is cast in terms of Brownian diffusions implicitly assume that correlations exist at infinitesimal scales. In the real-world where processes can only be observed discretely (and on finite time scales), if such a model is a plausible representation of the true data generating process, one should expect that empirical correlations can be recovered at all sampling scales—provided a sufficiently long series is available. As a consequence, the Epps effect would constitute a bias which requires correction.

In contrast, the fine-to-coarse model proposed by Bacry et al. (2013a) using a mutually exciting Hawkes process implicitly assumes that correlations depend on the sampling interval Δt . Therefore the Epps effect is a genuine effect and we only need to correct for statistical causes leading to an additional decay in correlations. The Epps effect is observed in nature, thus determining which abstract specification is a more realistic representation of the underlying data generating process is not merely a theoretical argument—it has practical significance. In particular, this has implications for the measurement and subsequent application of covariance/correlation matrices in high frequency contexts, as well as the meaningfulness and ability to extended high frequency estimates to and from different time scales. Indeed, this provides concerns about whether it is even possible to exploit any abundances of high frequency data in

Email addresses: patrick.chang@eng.ox.ac.uk (Patrick Chang),
etienne.pienaar@uct.ac.za (Etienne Pienaar),
tim.gebbie@uct.ac.za (Tim Gebbie)

order to improve estimates of such statistical properties as compared to low frequency counterparts.

It may appear difficult to determine whether a model is good or not, but we can determine the usefulness of a model in its ability to recover certain stylised facts and interrogate these by obtaining results from simulations that line up with what is seen empirically. In our case, a good model should be able to recover the Epps effect in its entirety. This has been problematic in the literature where the underlying representation or model data generating process if you will is based purely on Brownian diffusion specifications (see Münnix et al. (2011)). Brownian diffusions only explain a fraction of the empirically observed Epps effect and thus additional *ad hoc* complexity such as market microstructure noise (*i.e.* latent models where the observed process consists of a diffusion process with noise added to the trajectory, with the diffusion thus being treated as a latent component, see Aït-Sahalia et al. (2011) and Zhang (2010)) have been included in the modelling to try and conform the models with observations. Our concern with these specifications is that it may conceal the possibility of an inappropriate underlying representation. This may be detrimental when trying to correctly estimate covariance/correlation matrices with high frequency data as this can inadvertently lead to sub-optimal risk decisions.

This can be of particular concern if correlations are an emergent property dependent on time scales, rather than being a fundamental property imposed by the models used. If this is the case then correlations can be the result of complexity and collective interactions dynamically aggregated in a way that cannot always be faithfully represented by traditional stochastic processes, even with clever sampling or additional sources of noise and complexity. The impact of the choice and specification of time scales when making decisions predicated on estimates of correlation matrices can be of particular importance if there is a hierarchy of causal scales within the high frequency domain (Hendricks et al., 2016).

The Epps effect is pervasive and has been observed in stock markets and foreign exchange markets (see Mastromatteo et al. (2011) and references therein). The literature has isolated three primary potential sources: (i) asynchrony, (ii) lead-lag and (iii) tick-size. Concretely, Renò (2003) explored the effect of asynchrony under the presence of lead-lag. Precup and Iori (2007) demonstrated the impact different levels of asynchrony has on the Epps effect. Around the same time, Tóth and Kertész (2007) derived an analytical expression characterising the Epps effect as a function of the rate from the Poisson sampling. This led to the realisation that one can decompose the correlation at time interval Δt as a function of the correlation at a smaller time interval Δt_0 (Tóth and Kertész, 2009). Subsequently, Münnix et al. (2010) investigated the direct impact of tick-size on the Epps effect. They were able to find a representation that combined the compensation of tick-size with asynchrony (Münnix et al., 2011). The analytical expression characterising the Epps effect in Tóth and Kertész (2007) was then further extended by Mastromatteo et al. (2011) to separate the effects from asynchrony and that of lead-lag. More recently, Chang et al. (2021) investigated the Epps effect under different definitions of time.

Asynchrony is a statistical cause contributing to a decay in correlations as the sampling interval decreases. Many methods have been proposed to fix or compensate for this. The canonical approach of Hayashi and Yoshida (2005) propose a cumulative covariance estimator. Buccheri et al. (2019) characterised the Epps effect in terms of the probability of flat trading and provide a correction for the effect. Here we provide a correction based on the distortion resulting from partial overlapping intervals from the sampling process using the insights and innovations of Tóth and Kertész (2007), Mastromatteo et al. (2011) and Münnix et al. (2011). Methods aimed at compensating the effect due to asynchrony all assume that there is some underlying synchronous process with some true correlation for which we are interested in. Our concern is with the underlying representation of the synchronous process itself.

We demonstrate that the *residual Epps effect*, the remaining Epps effect after correcting for statistical causes, can allow us to discriminate between a diffusion-based representation for the underlying process and a diffusion-based process with *ad hoc* noise or discrete connected events. Currently we cannot discriminate between diffusion-based processes with *ad hoc* noise against discrete connected events. This is because both of these processes lead to similar behaviour in the residual Epps effect, albeit for completely different reasons. Nonetheless, we highlight the importance of finding the correct representation and argue that the Hawkes representation is likely more appropriate since it does not require *ad hoc* model complexity to recover the observed phenomenology.

The paper proceeds as follows. Section 2 demonstrates how the Epps effect arises from asynchrony. We introduce three methods to compensate for this effect. Section 3 we introduce the Hawkes process and its properties. Section 4 compares the various corrections for asynchrony under different underlying representations. Section 5 demonstrates how we can use the residual Epps effect to discriminate the underlying process. Section 6 discusses the limitations of our discrimination and the importance of finding the correct representation. Section 7 we discriminate the underlying representation on trade and quote data from the Johannesburg Stock Exchange (JSE). Finally, we end with some closing remarks in section 8.

2. Asynchrony: Compensating for the Epps effect

2.1. The Epps effect from asynchrony

Consider a multivariate diffusion process as the underlying representation of the stochastic nature of a log-price of the i th asset at time t . Assuming that the process has stationary increments dX_t^i , let the finite variation over the interval Δt be given by

$$X_{\Delta t}^i = \int_0^{\Delta t} dX_t^i.$$

The infinitesimal lagged correlation between asset i and j are taken to be

$$\langle dX_t^i dX_{t'}^j \rangle = c_{t-t'}^{ij} dt dt', \quad (1)$$

where $c_{t-t'}^{ij}$ is defined as

$$c_{t-t'}^{ij} = \begin{cases} \delta_{t-t'} & \text{if } i = j, \\ c\delta_{t-t'} & \text{if } i \neq j, \end{cases}$$

and δ_x denotes the delta function (unit impulse) at 0. This means δ_x is equal to 1 when $x = 0$ and is equal 0 when $x \neq 0$. We want to examine the behaviour of the covariance process $C_{\Delta t}^{ij} = \langle X_{\Delta t}^i X_{\Delta t}^j \rangle$ on time scales Δt . This can be computed using (1) as

$$C_{\Delta t}^{ij} = \int_0^{\Delta t} \int_0^{\Delta t} c_{t-t'}^{ij} dt dt'.$$

Following the double integration and unit impulse, it follows that for the synchronous case we have the variance and covariance as

$$C_{\Delta t}^{ii} = \Delta t \text{ and } C_{\Delta t}^{ij} = c\Delta t.$$

Thus the correlation of the synchronous process is

$$\rho_{\Delta t}^{ij} = \frac{C_{\Delta t}^{ij}}{\sqrt{C_{\Delta t}^{ii} \cdot C_{\Delta t}^{jj}}} = c.$$

We see that for the synchronous process both the variance and covariance scale linearly with the sampling interval Δt . Thus the correlation is independent of Δt . [Mastromatteo et al. \(2011\)](#) characterize the Epps effect by saying that the Epps effect is present whenever $\rho_{\Delta t}^{ij}$ depends on Δt and is absent otherwise.

A property of high frequency finance is that tick-by-tick trades arrive in an asynchronous fashion following an arrival type representation where the inter-arrivals are not equidistant. The Epps effect arising from asynchrony is derived by synchronising the asynchronous observations using previous tick interpolation. To this end, let $U^i = \{t_k^i\}_{k \in \mathbb{Z}}$ be the set of asynchronous arrival times observed between $[0, T]$ for a realisation of the underlying synchronous process X_t^i . Using these two components we can construct the synchronised process

$$\tilde{X}_{\Delta t}^i = \int_{t_1^i}^{t_2^i} dX_t^i,$$

where $t_1^i = \max\{t_k^i \in U^i | t_k^i \leq 0\}$ and $t_2^i = \max\{t_k^i \in U^i | t_k^i \leq \Delta t\}$. The resulting synchronised process is piece-wise constant with jumps at $t_k^i \in U^i$. A comparison of the two process $X_{\Delta t}^i$ and $\tilde{X}_{\Delta t}^i$ can be seen in figure 1.

Given U^i and U^j , the covariance of the synchronised process can be defined as

$$\begin{aligned} \tilde{C}_{\Delta t}^{ij} &= \mathbb{E} \left[\langle \tilde{X}_{\Delta t}^i, \tilde{X}_{\Delta t}^j \rangle \Big|_{U^i, U^j} \right] \\ &= \mathbb{E} \left[\int_{t_1^i}^{t_2^i} \int_{t_1^j}^{t_2^j} c_{t-t'}^{ij} dt dt' \Big|_{U^i, U^j} \right] \\ &= c \cdot \mathbb{E} \left[\left| [t_1^i, t_2^i] \cap [t_1^j, t_2^j] \right| \right], \end{aligned} \quad (2)$$

where $\mathbb{E}[\cdot]$ is the expectation of the sampling process. Similarly, the variance is defined as

$$\tilde{C}_{\Delta t}^{ii} = \mathbb{E} \left[\left| [t_1^i, t_2^i] \cap [t_1^i, t_2^i] \right| \right].$$

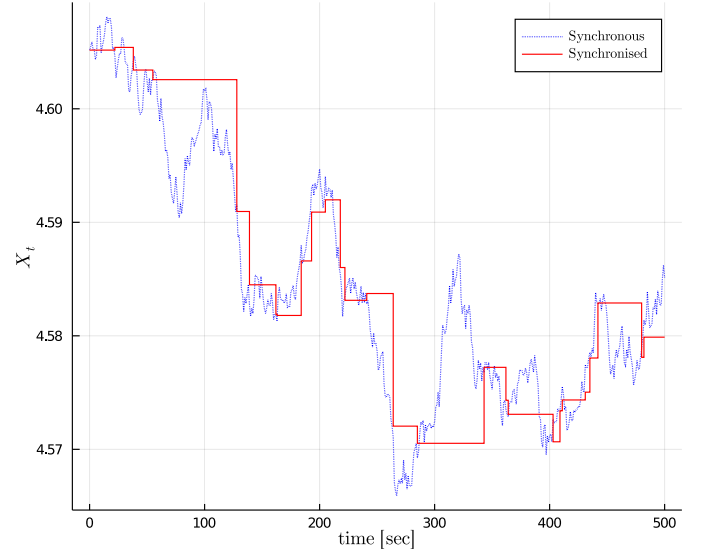


Figure 1: A comparison of a realisation of the synchronous process $X_{\Delta t}^i$ (dotted line) and the synchronised process $\tilde{X}_{\Delta t}^i$ (solid line). Here the inter-arrival distribution of U^i follows an exponential with $\lambda = 1/15$.

Given U^i and U^j , we can estimate the expectation of the overlap of the sampling process at a particular discretisation size Δt by defining a new variable $\gamma_i(t) = \max\{t_k^i : t_k^i \leq t\}$ for $t \in [0, T]$. The expectation can then be estimated as

$$\hat{\kappa}_{\Delta t}^{ij} = \mathbb{E} \left[\left| [\gamma_i(t - \Delta t), \gamma_i(t)] \cap [\gamma_j(t - \Delta t), \gamma_j(t)] \right| \right]. \quad (3)$$

Thus the correlation of the synchronised process is then given by

$$\tilde{\rho}_{\Delta t}^{ij} = c \cdot \frac{\hat{\kappa}_{\Delta t}^{ij}}{\sqrt{\hat{\kappa}_{\Delta t}^{ii} \cdot \hat{\kappa}_{\Delta t}^{jj}}}. \quad (4)$$

This depends on Δt and therefore the Epps effect is present.

The intuition is best explained by [Münnix et al. \(2011\)](#) and in (2). The correlation from the synchronous process $X_{\Delta t}$ is being extracted when the intervals $[t_1^i, t_2^i]$ and $[t_1^j, t_2^j]$ overlap, whereas the non-overlapping intervals are uncorrelated. Therefore the correlation of the synchronised process will be distorted by the non-overlapping intervals.

This approach has been previously investigated by [Tóth and Kertész \(2007\)](#), [Mastromatteo et al. \(2011\)](#) and [Münnix et al. \(2011\)](#). The key difference between the work of [Tóth and Kertész \(2007\)](#) and [Mastromatteo et al. \(2011\)](#) is that a specific distribution for the sampling process with stationary increments is chosen beforehand (usually a homogeneous Poisson). Here we only require that the sampling process have stationary increments. This can be useful because characterising the Epps effect with a specific *a-priori* distribution requires knowledge about the distribution of $\mathcal{W}_{\Delta t}$ defined as

$$\mathcal{W}_{\Delta t} = \min\{\gamma_i(t), \gamma_j(t)\} - \max\{\gamma_i(t - \Delta t), \gamma_j(t - \Delta t)\}.$$

This is not always easy to obtain. In the case of Poisson sampling we can find the exact distribution of $\mathcal{W}_{\Delta t}$ which means

(4) reduces to

$$\tilde{\rho}_{\Delta t}^{ij} = c \left(1 + \frac{1}{\lambda \Delta t} (e^{-\lambda \Delta t} - 1) \right). \quad (5)$$

There is a fundamental difference between our approach and that of Münnix et al. (2011). They compensate each of the overlapping return intervals while they are estimating the (compensated) correlation. In contrast, we separate the estimation of the correlation $\tilde{\rho}_{\Delta t}^{ij}$ and the compensation factor $\hat{\kappa}_{\Delta t}^{ij}$ as separate quantities. This is a crucial nuance that allows us to determine both the measured correlation from the synchronised process $\tilde{\rho}_{\Delta t}^{ij}$, and the corrected correlation from the synchronous process c . This is possible because our correction is performed after obtaining the measured correlation. Our correction is then easier to compute as we do not need to search for individual overlapping intervals to compensate.

2.2. Correcting for asynchrony

Here the Epps effect arises from sampling. For this reason the effect can be corrected. We proceed to discuss a few methods to do so. A key assumption underlying the correction is that there exists an underlying “true” and synchronous process which has some correlation quantity we are interested in. The observed samples are then merely realisations from this underlying process.

To measure the correlation $\tilde{\rho}_{\Delta t}^{ij}$ from the observables of the asynchronous process, we use previous tick interpolation coupled with the Realised Covariance (RC) estimator:

$$\tilde{\Sigma}_{T,\Delta t}^{ij} = \sum_{h=0}^{\lfloor T/\Delta t \rfloor} (\tilde{X}_{h\Delta t}^i - \tilde{X}_{(h-1)\Delta t}^i) (\tilde{X}_{h\Delta t}^j - \tilde{X}_{(h-1)\Delta t}^j).$$

The measured correlation is then

$$\tilde{\rho}_{\Delta t}^{ij} = \frac{\tilde{\Sigma}_{T,\Delta t}^{ij}}{\sqrt{\tilde{\Sigma}_{T,\Delta t}^{ii} \cdot \tilde{\Sigma}_{T,\Delta t}^{jj}}}. \quad (6)$$

Arrival time (overlap) correction:

The first correction method is to correct for the Epps effect directly from the characterisation of the synchronised process (4). To recover the correlation of the true synchronous process we compute:

$$\rho_{\Delta t}^{ij} = \tilde{\rho}_{\Delta t}^{ij} \cdot \frac{\sqrt{\hat{\kappa}_{\Delta t}^{ii} \cdot \hat{\kappa}_{\Delta t}^{jj}}}{\hat{\kappa}_{\Delta t}^{ij}}. \quad (7)$$

This defines the *overlap correction*. Here $\hat{\kappa}_{\Delta t}^{ij}$ can be directly estimated using U^i and U^j with discretisation size Δt .

Flat trade correction:

The second correction for the Epps effect is given by Buccheri et al. (2019). They take a different approach and assume that the process is observed at $n = \lfloor \frac{T}{\Delta t} \rfloor + 1$ non-random times equispaced over $[0, T]$, i.e. $0 < t_{0,n} < t_{1,n} < \dots < t_{n,n} = T$

where $\Delta t = t_{j,n} - t_{j-1,n}$ for $j \geq 1$. They then characterise the observables as

$$\tilde{X}_{t_{j,n}}^i = X_{t_{j,n}}^i (1 - B_{j,n}^i) + \tilde{X}_{t_{j-1,n}}^i B_{j,n}^i, \quad (8)$$

where $B_{j,n}^i$ are pairwise-independent triangular arrays of i.i.d. Bernoulli variables. The probability of flat trading is then $\mathbb{E}[B_{j,n}^i] = p_i$. In this setting they prove that the Realized Covariance estimator is biased (their Theorem 3.1) to then provide a correction

$$\rho_{\Delta t}^{ij} = \tilde{\rho}_{\Delta t}^{ij} \cdot \frac{(1 - \hat{p}_{\Delta t,i} \hat{p}_{\Delta t,j})}{(1 - \hat{p}_{\Delta t,i})(1 - \hat{p}_{\Delta t,j})}. \quad (9)$$

Here $\hat{p}_{\Delta t,i}$ is the estimate of the probability of flat trading p_i given by

$$\hat{p}_{\Delta t,i} = \frac{1}{\lfloor T/\Delta t \rfloor} \sum_{j=1}^{\lfloor T/\Delta t \rfloor} \mathbb{1}_{\{\tilde{X}_{j\Delta t}^i - \tilde{X}_{(j-1)\Delta t}^i = 0\}}, \quad (10)$$

where $\mathbb{1}$ is an indicator function. Convergence $\hat{p}_{\Delta t,i} \xrightarrow{p} p_i$ is then shown to hold.

We highlight that the assumptions used in Buccheri et al. (2019) are not always well suited for illiquid tick-by-tick trade data coupled with previous tick interpolation to achieve (8). Concretely, assumption 3 of their paper states that the maximum number of consecutive repeated trades is not large relative to the number of data points. This is because the price will only move to a new level when there is a new observable, and then all the grid points between observables will be flat trades. It is therefore difficult to satisfy assumption 3 using small grid points in illiquid markets with finite data.

Hayashi–Yoshida (baseline) correction:

Here the estimator corrects the effect by accounting for multiple contributions (Hayashi and Yoshida, 2005) and is defined by

$$\hat{\Sigma}_T^{ij} = \sum_{\ell=1}^{\#U^i} \sum_{k=1}^{\#U^j} (X_{t_\ell}^i - X_{t_{\ell-1}}^i) (X_{t_k}^j - X_{t_{k-1}}^j) \mathbb{1}_{\{(t_{\ell-1}, t_\ell] \cap (t_{k-1}, t_k] \neq \emptyset\}}, \quad (11)$$

where $\#U^i$ denotes the cardinality of the set U^i . The correlation is then given as

$$\rho^{ij} = \frac{\hat{\Sigma}_T^{ij}}{\sqrt{\hat{\Sigma}_T^{ii} \cdot \hat{\Sigma}_T^{jj}}}. \quad (12)$$

The Hayashi–Yoshida estimator is independent of the sampling interval Δt induced by the estimator from discretising the process into a synchronised process (performed using previous tick interpolation for the RC estimator). This is because (11) uses the synchronous process X_t^i where the times correspond to asynchronous transaction times given by the set of arrivals U^i . There is no re-sampling or discretisation that induces a time scale Δt . This means that we cannot use the estimator to investigate the correlations at a specific time scale Δt . The estimator is independent of Δt induced by the estimator. For this reason we will use it as a *baseline correction* for comparison.

The estimator is not independent from the sampling frequencies because it depends on the frequency of arrivals U^i . This means that the estimator can be used to investigate different time scales induced by the observables using, for example, k -skip sampling. However, it then becomes unclear what time scale Δt the estimator is recovering. Section 5 will discuss the two time scales in more detail.

Although we do not deal with lead-lag, we highlight that the Hayashi–Yoshida estimator cannot account for lead-lag as it assumes that the correlation between two assets do not extend beyond the interval with full or partial overlap (Griffin and Oomen, 2011).

3. Hawkes process

Hawkes (1971) introduced a class of multivariate point process allowing for event-occurrence clustering through a stochastic intensity vector. The stochastic intensity is composed from an *exogenous* or *baseline intensity* component which is not influenced by prior events and an *endogenous* component where prior events lead to an increased intensity. Within the endogenous component, *self-excitation* refers to an event type leading to more of the same event and *mutual-excitation* is an event driving the occurrence of other event types. Financial applications of the Hawkes process are plentiful. For a detailed review see Hawkes (2018) and Bacry et al. (2015). The application of the Hawkes process here is to construct a price model from bottom-up events and to model the arrival of asynchronous trades.

We consider the M -variate counting process $N(t) = \{N_m(t)\}_{m=1}^M$ with intensity $\lambda(t) = \{\lambda^m(t)\}_{m=1}^M$:

$$\lambda^m(t) = \lambda_0^m(t) + \sum_{n=1}^M \int_{-\infty}^t \phi^{mn}(t-s) dN_s^n,$$

where $\lambda_0^m(t)$ is the time dependent baseline intensity for the m -th component and $\phi^{mn}(t)$ is the kernel function which governs the dependency of prior events to the current time t . The kernel functions $\Phi(t) = \{\phi^{mn}(t)\}_{m,n=1}^M$ are (Bacry et al., 2015): (i) component-wise positive, (ii) component-wise causal and (iii) each component $\phi^{mn}(t)$ belongs to the space of L^1 -integrable functions. Popular kernels include the exponential kernel and the power law kernel (Bacry et al., 2015). We consider the simplest case of the Hawkes process used by Bacry et al. (2013a): a constant baseline intensity λ_0^m and exponential kernel given as $\phi^{mn}(t) = \alpha^{mn} e^{-\beta^{mn} t} \mathbb{1}_{t \in \mathbb{R}^+}$. Here α^{mn} and $\beta^{mn} > 0$ ensure that the Hawkes process is well defined.

The matrix of *branching ratios* are $\Gamma = \|\Phi\| = \{\|\phi^{mn}\|\}_{m,n=1}^M$, where $\|\phi^{mn}\|$ denotes the L^1 -norm defined as $\int_0^\infty \phi^{mn}(t) dt$. For the exponential kernel we have $\Gamma = \{\alpha^{mn} / \beta^{mn}\}_{m,n=1}^M$. The spectral radius of matrix Γ is defined as $\rho(\Gamma) = \max_{a \in \mathcal{S}(\Gamma)} |a|$ where $\mathcal{S}(\Gamma)$ is the set of all eigenvalues of Γ . The three phases of a Hawkes process are when $\rho(\Gamma) > 1$, $\rho(\Gamma) = 1$ and $\rho(\Gamma) < 1$. These correspond to the cases when the Hawkes process is *non-stationary*, *quasi-stationary* and *stationary* respectively. If the spectral radius of Γ is strictly less than one then the process is

stationary. The stationary condition ensures that the process remains *sub-critical* and will not lead to an explosion. Further details can be found in section 2.3.7 of Bacry et al. (2015).

Simulation is performed using the thinning procedure in appendix A of Toke and Pomponio (2012). The thinning procedure can be summarised as follows: let $I^K(t) = \sum_{k=1}^K \lambda^k(t)$ and let t be the current time. We sample an exponential inter-arrival time with rate parameter $I^K(t)$, call it τ . A random uniform u is then sampled from $[0, I^K(t)]$ and if $u < I^K(t) - I^K(t + \tau)$ then the arrival time $t + \tau$ is rejected. Otherwise the arrival time $t + \tau$ is accepted and attributed to the i th component where i is such that $I^{i-1}(t + \tau) < u \leq I^i(t + \tau)$.

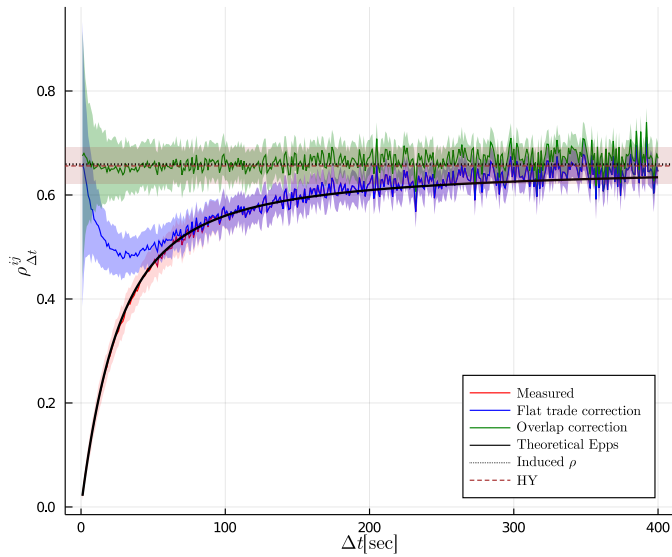
4. Simulation Experiments

The experiments focus on comparing the correction of the Epps effect arising from asynchrony from two types of sampling. The first from a homogeneous Poisson process (*Poisson sampling*) and the second from a 2-dimensional Hawkes process (*Hawkes sampling*). The sampling methods are performed on three types of price models. The first is a standard Brownian price model, the second is a stochastic volatility model contaminated with additive noise and the third is the Hawkes price model of Bacry et al. (2013a).

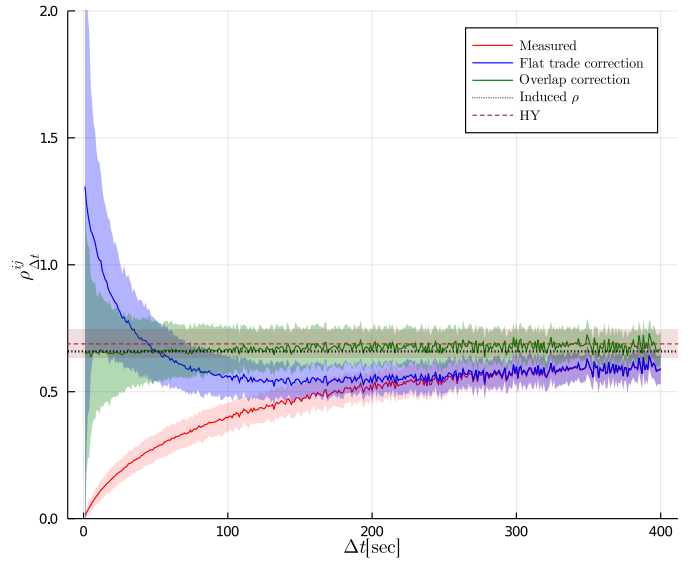
The experiments are conducted using simulated paths where T is 20 hours (72,000 seconds). The correlations will be investigated at small intervals where Δt is measured in seconds. The experiments use a single realisation of the price paths.¹ This is for two reasons. First, this emulates the circumstance with real data where we only have a single realisation. Second, this allows us to focus only on the effect of asynchrony when constructing the error ribbons and ensures that we do not conflate the effect of asynchrony with the sample specific variations from different price paths.

Each price path is then re-sampled using either a Poisson or Hawkes sampling scheme for 100 replications. The figures plot the mean estimate at each Δt over 100 replications for the various correlation and correction estimates. The error ribbons contain 95% of the estimates at each Δt from the replications computed using the Student t -distribution with 99 degrees of freedom and the standard deviation of the estimates between the replications at each Δt .

Our simulations have two types of sampling. First is the sampling of the synchronous process using Poisson or Hawkes sampling to obtain the observables. Second is the sampling from the observables using previous tick interpolation at a particular Δt to create a synchronised process to estimate the measured correlation (6) for the overlap correction (7) and the flat trade correction (9). The two types of sampling relate to *two time scales* induced by the observables and estimators respectively; this is discussed in greater detail in section 5.



(a) Brownian price model with Poisson sampling



(b) Brownian price model with Hawkes sampling

Figure 2: A Brownian price model with (a) Poisson sampling and (b) Hawkes sampling is presented: the red line is the measured correlation from the synchronised process (6), the blue line is the flat trade correction (9) and the green line is the overlap correction (7). The black line is the plot of (5). The horizontal dotted line is the induced correlation of the synchronous system with $\rho \approx 0.65$. Lastly the horizontal dashed line is the Hayashi–Yoshida estimate (12).

4.1. Brownian price model

Consider a standard Brownian log-price model satisfying the following SDEs:

$$\begin{aligned} dX_t^1 &= \left(\mu_1 - \frac{\sigma_1^2}{2} \right) dt + \sigma_1 dW_t^1, \\ dX_t^2 &= \left(\mu_2 - \frac{\sigma_2^2}{2} \right) dt + \sigma_2 dW_t^2. \end{aligned}$$

Here the infinitesimal correlation between dW_t^1 and dW_t^2 is ρ^{12} , and is set to be approximately 0.65.² The process is simulated using the Euler–Maruyama scheme with the discretisation size corresponding to one second intervals. The parameters used are $\mu_1 = \mu_2 = 0.01$, $\sigma_1^2 = 0.1$ and $\sigma_2^2 = 0.2$ (given in daily intervals). The first 500 seconds of this process is shown in figure 1.

To obtain the observables, this process is then sampled using a Poisson process with a mean inter-arrival of $1/\lambda = 15$ seconds and a 2-dimensional Hawkes process with $\lambda_0^1 = \lambda_0^2 = 0.015$ and Φ taking the form

$$\Phi = \begin{pmatrix} 0 & \phi^{(s)} \\ \phi^{(s)} & 0 \end{pmatrix}, \quad (13)$$

where $\phi^{(s)} = 0.023e^{-0.11t} \mathbb{1}_{t \in \mathbb{R}^+}$.

Figure 2 compares the correction methods for (a) Poisson and (b) Hawkes sampling on the Brownian price model. The overlap correction and the Hayashi–Yoshida estimator correctly recovers the underlying correlation of the synchronous process.

¹Indeed, one could simulate many paths, but that this is not expected to change the results beyond enhancing this error ribbons.

²The value is chosen for suitable comparison against the limiting correlation of the Hawkes price model in section 4.3.

What is interesting is that the flat trade correction does not recover the induced underlying correlation and the correction returns estimates outside the feasible range for correlations under the Hawkes sampling.³

This is curious because the estimator is in fact a consistent estimator as proved by Buccheri et al. (2019). We suspect that the cause of this is due to the long inter-arrivals from our sampling of the observables coupled with a small discretisation size Δt from the previous tick interpolation which leads to extended periods of flat trading. These extended period of flat trading makes the estimates of flat trade correction (10) closer to one. This leads to two possible reasons as to why the underlying correlation is not recovered. First, the variance of the flat trade correction spikes when the probability of flat trading p_i are simultaneously close to one (see figure 3 of Buccheri et al. (2019)). Second, the high probability of flat trading may possibly lead to too many consecutive flat trades which can violate assumption 3 in Buccheri et al. (2019).

The theoretical Epps effect arising from asynchrony (thick solid line) is plotted for the Poisson sampling since the distribution of $\mathcal{W}_{\Delta t}$ can be recovered in this case. Thus the theoretical Epps effect is given by (5). This theoretical Epps effect is not plotted for the Hawkes sampling as obtaining the distribution of $\mathcal{W}_{\Delta t}$ is not simple in this case. The main feature behind our correction method is that we do not need to obtain the distribution of $\mathcal{W}_{\Delta t}$ since the correction can be directly estimated using (3) given U^i and U^j .

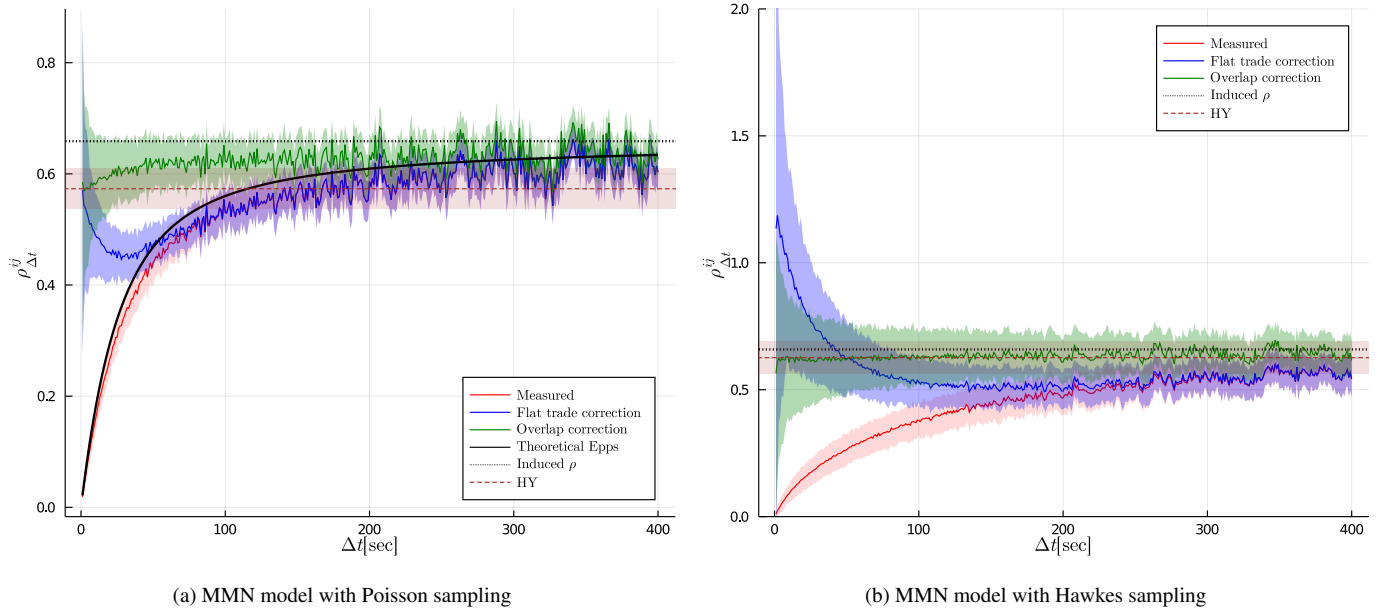


Figure 3: A market microstructure noise model with (a) Poisson sampling and (b) Hawkes sampling is presented: the red line is the measured correlation from the synchronised process (6), the blue line is the flat trade correction (9) and the green line is the overlap correction (7). The black line is the plot of (5). The horizontal dotted line is the induced correlation of the synchronous system with $\rho \approx 0.65$. Lastly the horizontal dashed line is the Hayashi–Yoshida estimate (12).

4.2. Market microstructure noise model

Consider a more complex *ad hoc* model that is still predicated on Brownian motions. We consider a log-price model where the synchronous process X_t^i has been contaminated with additive noise:

$$\begin{aligned} X_t^1 &= P_t^1 + \epsilon_t^1, & \epsilon_t^1 &\sim \text{NID}(0, h_1^2), \\ X_t^2 &= P_t^2 + \epsilon_t^2, & \epsilon_t^2 &\sim \text{NID}(0, h_2^2), \end{aligned}$$

where ϵ_t^i is normal white noise that captures market microstructure effects. Here we assume that the latent process P_t^i satisfies the following SDEs:

$$\begin{aligned} dP_t^1 &= \sigma_{t,1} dW_t^1, \\ dP_t^2 &= \sigma_{t,2} dW_t^2, \end{aligned}$$

where the infinitesimal correlation between dW_t^1 and dW_t^2 is ρ^{12} , and is set to be approximately 0.65. Here $\sigma_{t,i}$ is a time varying standard deviation that can be decomposed as

$$\sigma_{t,i} = d_t g_{t,i},$$

where d_t is a common diurnal pattern given by

$$d_t = C + Ae^{-at} + Be^{-b(1-t)}$$

and $g_{t,i}$ evolves according to

$$dg_{t,i}^2 = k_i(v_i - g_{t,i}^2)dt + w_i g_{t,i} dB_t^i.$$

³None of the correction methods guarantee that the corrected estimates for the correlation lie within $[-1, 1]$.

This model will be henceforth referred to as the market microstructure noise (MMN) model.⁴ The process is simulated using the Euler–Maruyama scheme with the discretisation size corresponding to one second intervals. The parameters $A = 0.75$, $B = 0.25$ and $C = 0.88929198$ are set in a way such that $1/T \left(\int_0^T d_t^2 dt \right) = 1$. The remaining parameters are set as $v_1 = 0.01$, $v_2 = 0.02$, $w_1 = w_2 = 0.1$ and $k_1 = k_2 = 10$. The average signal-to-noise ratio between v_i and h_i^2 is set to be one-to-one and the leverage effect between dB_t^i and dW_t^i is set to be 0.01.

To obtain the observables, we sample the MMN model with a Poisson process with a mean inter-arrival of $1/\lambda = 15$ seconds and a 2-dimensional Hawkes process taking the form of (13) with parameters $(\lambda_0^1 = \lambda_0^2, \alpha^{(s)}, \beta) = (0.015, 0.023, 0.11)$.

Figure 3 compares the correction methods for (a) Poisson and (b) Hawkes sampling on the MMN model. We see that in figure 3(a) that all the estimates are lower compared to the estimates from figure 2(a). The lower correlation achieved is a result of the contamination from noise. It is a well known result that the realised volatility estimator overestimates the volatility when the process is contaminated with additive noise (Zhang et al., 2005). This increased volatility estimate leads to a larger normalisation factor and thus the correlation estimates are lower than before.

What is interesting is that the estimates in figure 3(b) are not as affected by noise when compared to figure 3(a). The reason behind this is because the specification of the Hawkes sampling in (13) results in longer inter-arrivals compared to the Poisson

⁴This is the same model used in Buccheri et al. (2020) but without lead-lag components.

sampling. This hints towards the fact that the time scale induced by the observables play a role in our ability to correct for asynchrony. This result forms the basis for our ability to discriminate between the processes which we will discuss in section 5.

4.3. Hawkes price model

Consider the price model introduced by Bacry et al. (2013a) constructed using interconnected events from a Hawkes process. Let the bivariate log-price be

$$\begin{aligned} X_t^1 &= X_0^1 + N_1(t) - N_2(t), \\ X_t^2 &= X_0^2 + N_3(t) - N_4(t), \end{aligned}$$

where $\{N_m(t)\}_{m=1}^4$ is a 4-dimensional mutually exciting Hawkes process with the kernel Φ taking the form:

$$\Phi = \begin{pmatrix} 0 & \phi^{(r)} & \phi^{(c)} & 0 \\ \phi^{(r)} & 0 & 0 & \phi^{(c)} \\ \phi^{(c)} & 0 & 0 & \phi^{(r)} \\ 0 & \phi^{(c)} & \phi^{(r)} & 0 \end{pmatrix}. \quad (14)$$

The interpretation of kernel components in (14) is as follows: $\phi^{(r)}$ imitates mean reversion because an uptick in X^1 by N_1 will lead to an increased intensity in the down tick N_2 —allowing the price level to revert (similarly for X^2 through N_3 and N_4). On the other hand $\phi^{(c)}$ induces a correlation between the prices by connecting the two prices since an uptick in X^1 by N_1 will lead to an increased intensity in the uptick of X^2 through N_3 (similarly for down ticks through N_2 and N_4).

We use the same specification and parameters as Bacry et al. (2013a) for the construction of kernel in (14) with $\lambda_0^m = \mu, \forall m$, $\phi^{(r)} = \alpha^{(r)} e^{-\beta t} \mathbb{1}_{t \in \mathbb{R}^+}$ and $\phi^{(c)} = \alpha^{(c)} e^{-\beta t} \mathbb{1}_{t \in \mathbb{R}^+}$. Therefore the parameters are given as $(\mu, \alpha^{(r)}, \alpha^{(c)}, \beta) = (0.015, 0.023, 0.05, 0.11)$.

Figure 4 plots a single realisation for the price model. It is clear that figure 4(a) looks like a diffusive model such as that in figure 1. However, from figure 4(b) we clearly see the jumps and that the price model is composed of discrete events. Over long horizons these events start behaving like diffusion processes. Limit theorems for Hawkes price models have been derived by Bacry et al. (2013b).

A key insight from Bacry et al. (2013a) is their formulation of the Epps effect using the Hawkes price model where they derive the covariance matrix as a function of Δt

$$\begin{aligned} \frac{C_{\Delta t}^{11}}{\Delta t} &= \Lambda + \frac{RC_1}{2G_1} + \frac{RC_2}{2G_2} \\ &+ R \frac{C_2 G_1^2 e^{-\Delta t G_2} - C_1 G_2^2 + Q_1 G_2^2 e^{-\Delta t G_1} - C_2 G_1^2}{2G_2^2 G_1^2 \Delta t}, \end{aligned}$$

and

$$\begin{aligned} \frac{C_{\Delta t}^{12}}{\Delta t} &= \frac{-RC_1}{2G_1} + \frac{RC_2}{2G_2} \\ &+ \frac{R(C_1 G_2^2 - C_2 G_1^2 - C_1 G_2^2 e^{-G_1 \Delta t} + C_2 G_1^2 e^{-G_2 \Delta t})}{2G_2^2 G_1^2 \Delta t}. \end{aligned}$$

Here the parameters are:

$$\begin{aligned} \Lambda &= \frac{\mu}{1 - \Gamma_{12} - \Gamma_{13}}, \\ R &= \frac{\beta \mu}{\Gamma_{12} + \Gamma_{13} - 1}, \\ C_1 &= \frac{(2 + \Gamma_{12} + \Gamma_{13})(\Gamma_{12} + \Gamma_{13})}{1 + \Gamma_{12} + \Gamma_{13}}, \\ C_2 &= \frac{(2 + \Gamma_{12} - \Gamma_{13})(\Gamma_{12} - \Gamma_{13})}{1 + \Gamma_{12} - \Gamma_{13}}, \\ Q_1 = Q_4 &= \frac{-\mu(\Gamma_{12}^2 + \Gamma_{12} - \Gamma_{13}^2)}{((\Gamma_{12} + 1)^2 - \Gamma_{13}^2)(1 - \Gamma_{12} - \Gamma_{13})}, \\ Q_2 = Q_3 &= \frac{-\mu \Gamma_{13}}{((\Gamma_{12} + 1)^2 - \Gamma_{13}^2)(1 - \Gamma_{12} - \Gamma_{13})}, \end{aligned}$$

and

$$G_1 = \beta(1 + \Gamma_{12} + \Gamma_{13}), \quad G_2 = \beta(1 + \Gamma_{12} - \Gamma_{13}).$$

The underlying correlation for the synchronous Hawkes price model is then given by

$$\rho_{\Delta t}^{12} = \frac{C_{\Delta t}^{12}}{C_{\Delta t}^{11}}. \quad (15)$$

Moreover, in the limit we have (Bacry et al., 2013a)

$$\lim_{\Delta t \rightarrow \infty} \rho_{\Delta t}^{12} = \frac{2\Gamma_{13}(1 + \Gamma_{12})}{1 + \Gamma_{13}^2 + 2\Gamma_{12} + \Gamma_{12}^2}.$$

Figure 5 demonstrates the Epps effect arising from the Hawkes price model. A crucial feature that cannot be understated here is that the Epps effect arises from *synchronous* samples. There are no statistical causes such as asynchrony or tick-size nor is the effect of lead-lag contributing towards the Epps effect. Under this model it is more accurate to think of the Epps effect as the emergence of correlation as Δt increases rather than a decay in correlation. This is a crucial insight despite the conceptual simplicity of the model.

This is because at small time intervals the events are merely random. The connection between the events can only be detected when there are sufficient events in a given interval. Meaning that a system created by events takes a finite time to correlate and requires the concept of intervals to be externally imposed by an external observer to give the notion of correlation meaning. This is the fundamental difference between this model and those considered earlier. Correlation from the Hawkes price model is a result of the prices being coupled between discrete and connected events, whereas the models predicated on Brownian motions have an underlying correlation at infinitesimal scales written in *a-priori* by the system observers to then later be estimated and fitted to observed re-sampled data.

The observables are again obtained by sampling the Hawkes price model using a Poisson process with a mean inter-arrival of $1/\lambda = 15$ seconds and a 2-dimensional Hawkes process taking the form of (13) with parameters $(\lambda_0^1 = \lambda_0^2, \alpha^{(s)}, \beta) = (0.015, 0.023, 0.11)$.

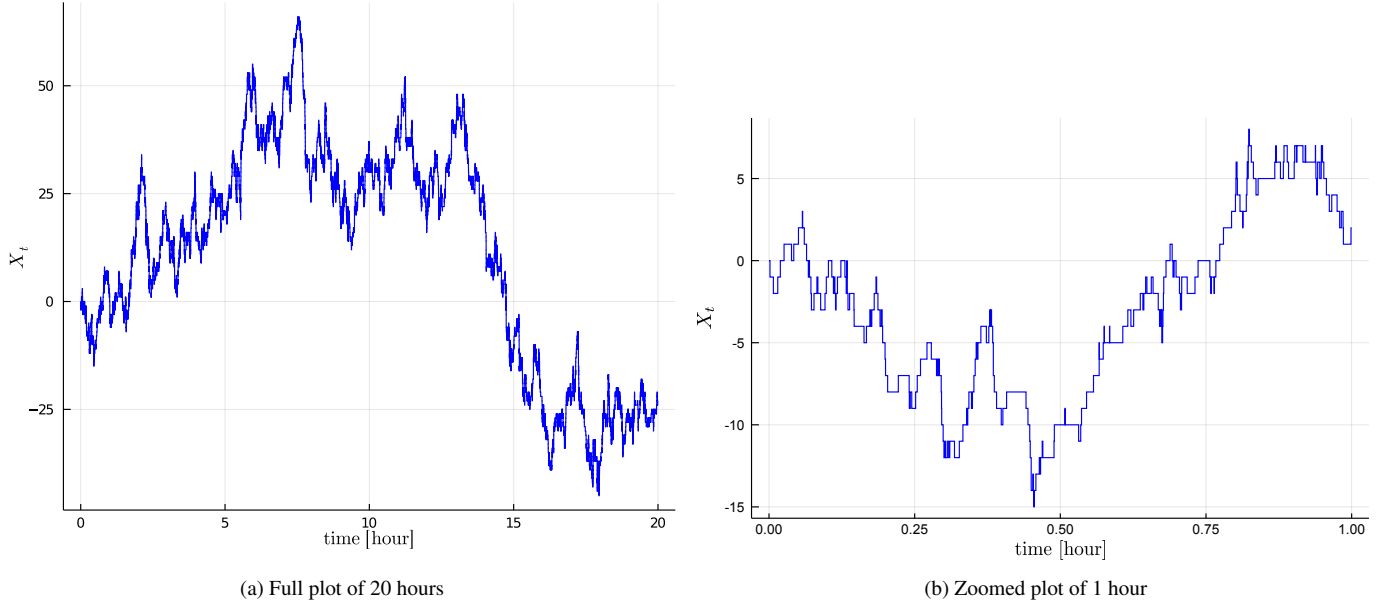


Figure 4: A Hawkes price model is plotted: (a) plots the full 20 hours where the path looks like that from a diffusion process and (b) zooms in the first hour where the jumps are clearly seen.

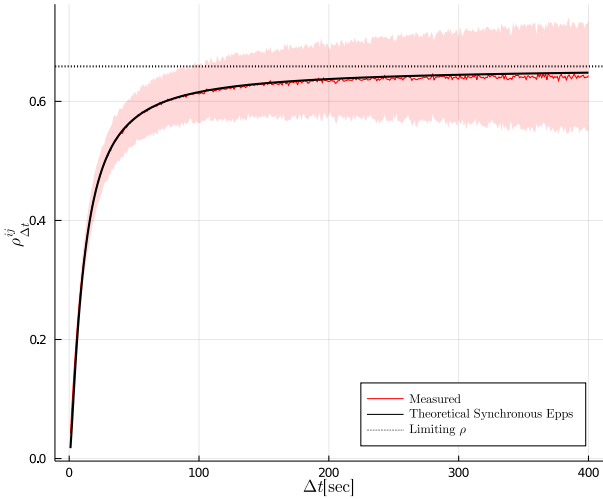


Figure 5: The Epps effect is demonstrated from the Hawkes price model where the red line is the measured correlation (6) from *synchronous* samples. The black line is the plot of (15) and the dotted horizontal line is the correlation as $\Delta t \rightarrow \infty$. Using the parameters $(\mu, \alpha^{(r)}, \alpha^{(c)}, \beta) = (0.015, 0.023, 0.05, 0.11)$ we have that $\rho_{\Delta t}^{12} \approx 0.65$ as $\Delta t \rightarrow \infty$.

Figure 6 compares the correction methods for (a) Poisson and (b) Hawkes sampling on the Hawkes price model. We see that the flat trade correction overcorrects the correlation for both cases. This is because the Hawkes price model only jumps to a new price state when an event occurs. Moreover, an uptick is likely followed by a down tick due to the mean reverting property. This interaction can lead to an amplification of an extended period of flat trades which results in the estimate of the probability of flat trading (10) being closer to one.

The measured correlation from the synchronised process

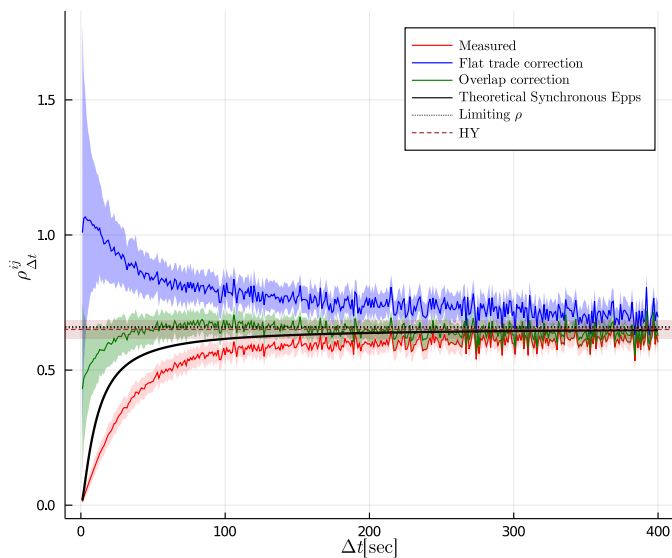
exhibits a further Epps effect relative to the theoretical synchronous Epps effect (thick line) which is expected. This difference is naturally attributed towards the asynchronous sampling.

What is interesting is that in both figures 6(a) and 6(b), the Hayashi–Yoshida estimates recover the limiting correlation but the overlap correction only recovers the limiting correlation in figure 6(b). The overlap correction in figure 6(a) under estimates the limiting correlation and over estimates the synchronous Epps effect. This is curious because if we are correcting for asynchrony then we should be recovering the correlation of the theoretical synchronous Epps effect. This hints again at the fact that the implicit time scales induced by the choices of observables play an important role in our ability to correct for asynchrony.

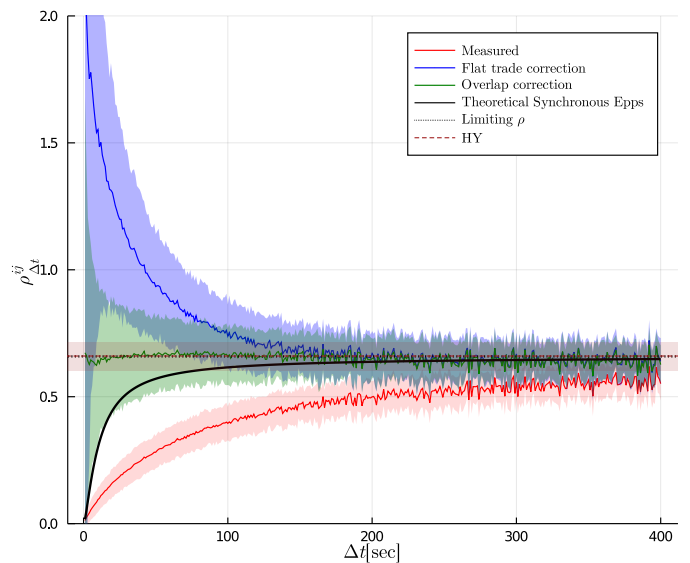
5. The residual Epps effect

The key realisation is that there are in fact at least two time scales at play. First is the time scale induced by the observables. In our experimental context this is the sampling of the synchronous process to obtain the observables. Second is the time scale induced by the estimator. This is induced by the previous tick interpolation at a particular discretisation size Δt to create a synchronised process.

Remark 1. *Previous tick interpolation is not the only way an estimator can induce a time scale. The Malliavin–Mancino Fourier estimator (Malliavin and Mancino, 2002, 2009) directly uses the observables without the need to create a synchronised process. However, the estimator induces a time scale through the number of Fourier coefficients of the price process it uses to estimate the Fourier coefficients of the volatility process (Chang et al., 2020). It is this property that Renò (2003)*



(a) Hawkes price model with Poisson sampling



(b) Hawkes price model with Hawkes sampling

Figure 6: The Hawkes price model with (a) Poisson sampling and (b) Hawkes sampling is presented: the red line is the measured correlation from the synchronised process (6), the blue line is the flat trade correction (9) and the green line is the overlap correction (7). The black line is the plot of (15). The horizontal dotted line is the limiting correlation when $\Delta t \rightarrow \infty$ which means $\rho_{\Delta t}^{12} \approx 0.65$. Lastly the horizontal dashed line is the Hayashi–Yoshida estimator (12).

and Precup and Iori (2007) exploit to investigate the Epps effect using the Malliavin–Mancino Fourier estimator.

The interplay between the two time scales and the underlying process will determine our ability to correct for asynchrony. Concretely, the time scale induced by the observables will not affect our ability to correct for asynchrony on the Brownian price model but it will affect our ability to correct for asynchrony on the MMN and Hawkes price model.

Experiment #1: Hayashi–Yoshida

Let us consider some additional experiments to demonstrate this point. The Hayashi–Yoshida estimator is a unique estimator in that it does not induce a time scale Δt when estimating the correlation. It recovers the underlying correlation directly from the observables. This gives us the ability to investigate the effect of the time scale induced by the observables without the interaction from the time scale induced by the estimator.

We simulate a single realisation of the price paths from each of the models investigated in section 4. The time scale induced by the observables are controlled using the Poisson sampling with the average inter-arrivals ranging from 1 to 45 seconds. Each price model is then re-sampled with the different average inter-arrivals 100 times. Figure 7 plots the mean Hayashi–Yoshida estimate on (a) the Brownian price model, (b) the MMN model and (c) the Hawkes price model as a function of the average inter-arrival time with error ribbons containing 95% of the estimates at each $1/\lambda$ over the 100 replications.

We see in figure 7 that the Hayashi–Yoshida estimator recovers the induced correlation of the Brownian price model regard-

less of the time scale induced by the observables.⁵ On the other hand we see that the estimator presents an Epps like effect as a function of the average inter-arrival time for the MMN and Hawkes price model.

However, the Epps like effect from the MMN and Hawkes price models arise because of very different reasons. The decay in correlations from the MMN model is a result of the signal-to-noise ratio at the different time scales induced by the observables. On shorter time scales the log-return observed from transactions is mostly composed of market microstructure noise and brings little information regarding the volatility of the price process, whereas on longer time scales the amount of market microstructure noise remains constant while the informational content of volatility increases (Ait-Sahalia et al., 2005). This leads to an overestimation of volatility on shorter time scales which results in the decay of correlations. On the other hand the Epps like effect from the Hawkes price model is the result of the observables inducing a different time scale average over the underlying events. This means we recover a correlation estimate from the synchronous process over a mixture of time scales from the observables.

This means we can discriminate the underlying process of an unknown system by re-sampling the process at different average inter-arrivals and estimating the Hayashi–Yoshida estimates.⁶ If the plot is flat for various values of $1/\lambda$ then the underlying

⁵Note that the discretisation in the simulation of the diffusion process should be finer than the average inter-arrivals to avoid insufficient granularity in the diffusion process.

⁶Our experiments are not formal hypothesis tests but a heuristic approach aimed at determining which implicit model assumption is better satisfied through the stylised facts.

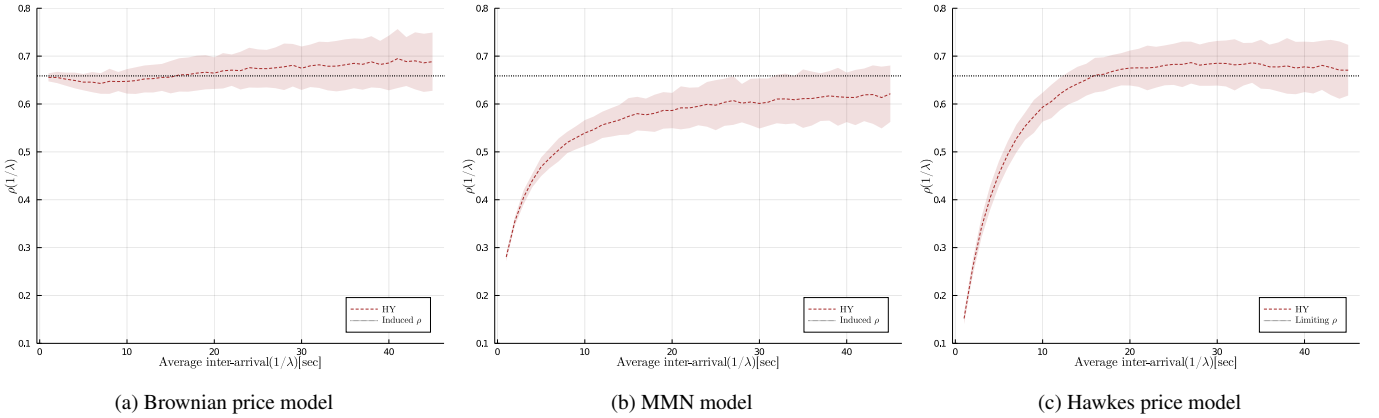


Figure 7: The Hayashi–Yoshida estimate (dashes lines) given in (12) plotted as a function of the mean inter-arrival for (a) the Brownian price model, (b) the MMN model and (c) the Hawkes price model. The limiting/induced ρ (horizontal dotted line) is approximately 0.65 as before. We see how the time scale induced by the observables can affect the correction of asynchrony for the different underlying processes.

process is a diffusion-based process. If the plot presents decaying correlation for smaller $1/\lambda$ then the underlying process is either a diffusion-based process but contaminated with *ad hoc* noise or it is composed of discrete connected events (a system where correlation is then emergent).

Experiment #2: Overlap correction

In the next experiment we plot the actual residual Epps curves which allows us to investigate the interplay between the two time scales induced by the observables and the estimator on the MMN and Hawkes price model. Once again the time scale induced by the observables are controlled using the Poisson sampling with average inter-arrivals set as $1/\lambda = 1, 10, 25$. In this case there is no need to perform the experiment with the Brownian price model. This is because with the Poisson sampling, the Epps effect is characterised exactly by (5) and therefore the residual Epps effect here will be flat and recover the correct underlying correlation for the various inter-arrivals.

In figure 8 we see that in both the MMN and Hawkes price model that the overlap correction tends towards the induced/limiting correlation as $1/\lambda$ increases, whereas the overlap correction presents the residual Epps effect as $1/\lambda$ decreases.

We see that our ability to recover the induced correlation becomes problematic when $1/\lambda$ becomes smaller for the MMN model. This is because the signal-to-noise ratio is larger on shorter time scales. On the other hand we see that we start to recover the correlation from the synchronous case when $1/\lambda$ is very small for the Hawkes model. This is expected since the asynchrony correction is supposed to recover the correlation from the synchronous process. This confirms that indeed the time scale induced by the observables do in fact play a fundamental role in our ability to correct for asynchrony.

This experiment also gives us a method to discriminate the underlying process of an unknown system. This is achieved by sampling the unknown system with different average inter-arrivals and then plotting the residual Epps curves using the overlap correction. If the residual Epps curves are flat for all values of $1/\lambda$ then the underlying process is a diffusion-based

process. If the residual Epps curves decay more for smaller $1/\lambda$ then the underlying process is either a diffusion-based process but contaminated with *ad hoc* noise or is composed of discrete connected events.

Experiment #3: *k*-skip Hayashi–Yoshida

The first two experiments are well suited to determine the underlying process of an unknown system in a simulation scenario. This is because the first two experiments require the re-sampling of the process to obtain different sets of observables U^i and U^j with different sized inter-arrivals. This is a problem with TAQ data because there is only one set of U^i and U^j . Moreover, the second experiment requires multiple replications to get a good gauge on the error ribbons. Using results based on one replication with the second experiment cannot meaningfully determine the underlying process. Error bands are required to clearly see that the process consistently decays. The first experiment does not require replications to determine the underlying process. This is because the error ribbons are very narrow. This means that the estimates are either flat or they decay.

This experiment is a variant of the first experiment but overcomes the issue of requiring multiple sets of U^i and U^j . This is achieved by using a single set of U^i and U^j when discriminating. Griffin and Oomen (2011) provided the inspiration to overcome this issue by using *k*-skip sampling. With only one set of arrivals U^i and U^j , we can imitate multiple sets of arrivals with different sized inter-arrivals by sampling every *k*th observation in the single set of arrivals. Concretely, from the single set of U^i , let the *k*th-skip set of samples be the set $U_k^i = \{t_k^i, t_{2k}^i, \dots, t_{\lfloor \#U^i/k \rfloor}^i\}$. Note that $\#U^i$ is the cardinality of set U^i . Instead of re-sampling and computing the Hayashi–Yoshida estimate with different mean inter-arrival $1/\lambda$, we can now compute the Hayashi–Yoshida estimate as a function of the *k*th-skip set of samples U_k^i and U_k^j .

Figure 9 plots the Hayashi–Yoshida estimates as a function of the *k*-skip sampling for (a) the Brownian price model, (b)

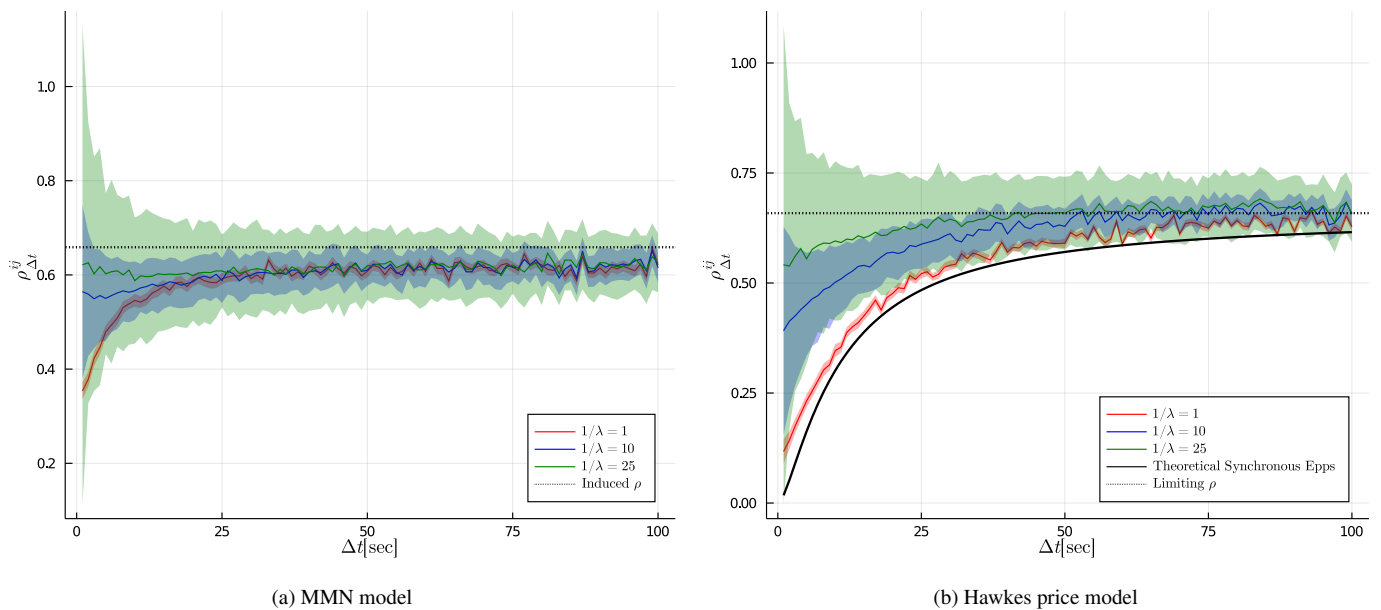


Figure 8: The overlap correction (7) for three sampling frequencies of observables are plotted. The three sampling frequencies chosen are: $1/\lambda = 1, 10, 25$ which corresponds to the red, blue, green lines respectively. The thick line is the theoretical synchronous Epps effect given by (15) and the horizontal dotted line is the induced/limiting ρ set to be approximately 0.65 as before. We see the interplay between the time scale induced by the observables and the time scale induced by the estimator.

the MMN model and (c) the Hawkes price model. The k -skip sampling is performed by sampling every observation $k = 1$ to every 50th observation $k = 50$. To re-create conditions similar to that of empirical data, we only sample one set of observables from each price process. Figure 9 recovers similar results as figure 7. We see that the induced correlation of the Brownian price model is recovered for any sized k -skip sampling, whereas the MMN and Hawkes price model presents an Epps like effect as a function of the k -skip sampling.

This result allows us to discriminate the underlying process of an unknown system with one set of observables. If the plot is flat for various values of k then the underlying process is a diffusion-based process. If the plot presents a decaying correlation for smaller k then the underlying process is either a diffusion-based process but contaminated with *ad hoc* noise or is simply composed of discrete connected events.

6. Perspectives on noise and discreteness

Limitations of the discrimination

In section 5 we were able to discriminate a diffusion-based process against diffusion-based processes with *ad hoc* noise, or discrete connected events. However, we cannot discriminate between diffusion-based processes with *ad hoc* noise and discrete connected events. This is because both of these processes lead to similar behaviour in the residual Epps effect, albeit for completely different reasons.

In order to discriminate between these two processes we need better estimators or better experiments. In appendix Appendix A we applied two alternative estimators to demonstrate the complexity and ambiguity relating to attempts to discriminate

between the MMN and Hawkes price model using the second experiment.

Specifically, we applied the Quasi-Maximum Likelihood Estimator (QMLE) by Ait-Sahalia et al. (2010) and the Kalman-EM (KEM) estimator by Corsi et al. (2015) to the problem. We find that both processes lead to similar behaviours in the residual Epps effect and it remains unclear on how we can discriminate between these the processes.

Another possible limitation of our experiments is that they are not designed to account for lead-lag. This could be problematic because Griffin and Oomen (2011) recovered similar behaviour that was found in figures 9(b) and 9(c) using empirical TAQ data from the New York Stock Exchange (NYSE) with the k -skip Hayashi–Yoshida estimator. However, they argue that empirical data has a sluggish behaviour for price adjustments to reflect the appropriate correlation. Therefore this behaviour demonstrates a problem with the Hayashi–Yoshida estimator because the underlying assumption of the estimator assumes that all available information regarding the correlation should be fully incorporated when a price update arrives. They then correct for this by adjusting the Hayashi–Yoshida estimator to account for lead-lag dependencies.

Lead-lags can arise within the framework of the Hawkes price model by Bacry et al. (2013a,b), however the specification used here in (14) is fully symmetric and thus there are no lead-lag effects in our models (see Bacry et al. (2013a) and Remark 9 of Bacry et al. (2013b)). Currently our discrimination is performed without considering lead-lag effects but this is something that should be incorporated when designing future experiments.

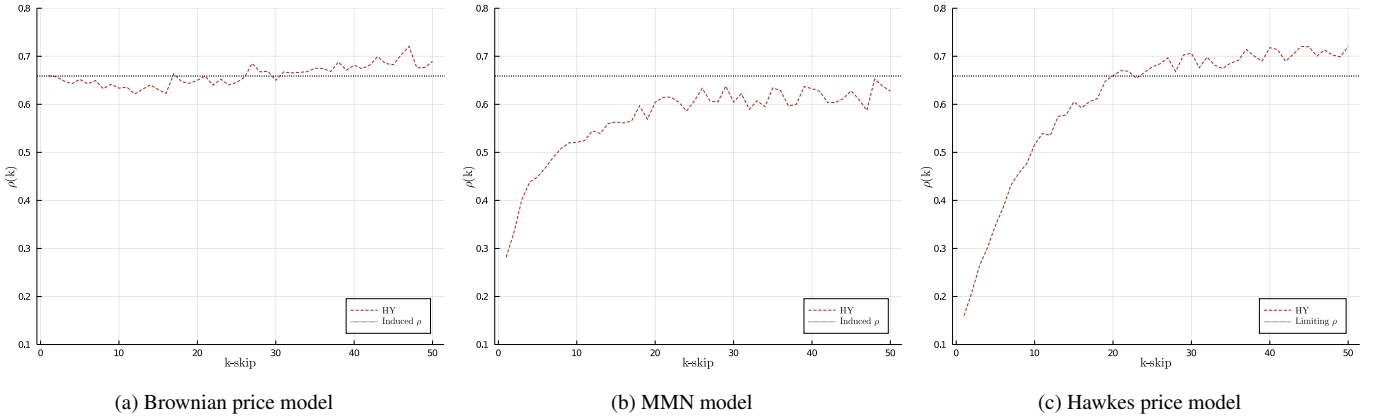


Figure 9: The Hayashi–Yoshida estimate (dashed lines) given in (12) plotted as a function of the k -skip sampling for (a) the Brownian price model, (b) the MMN model and (c) the Hawkes price model. The limiting/induced ρ (horizontal dotted line) is approximately 0.65 as before. We see that k -skip sampling allows us to discriminate the processes with one set of arrivals.

Finding the correct representation

Intraday financial prices are subject to discretisation effects where the prices are multiples of the tick-size. This is a fundamental property of financial markets arising from how financial markets are designed. This discrete nature of financial markets is naturally incorporated within tick-by-tick models such as the Hawkes price model. However, this effect poses a problem to macroscopic models such as those built using Brownian diffusions because it affects the estimation of correlations (Münnix et al., 2011).

The provocatively named “market microstructure effect” was introduced to reconcile macroscopic models with the signature plot (Aït-Sahalia et al., 2005, 2011; Zhang et al., 2005). It is modelled through noise to capture various microstructure effects such as the discreteness of price changes, bid-ask bounces and measurement or rounding errors. However, we argue that the main purpose behind noise is to reconcile the discrepancy between the fundamental tick-by-tick nature of financial markets and the macroscopic models used (Aït-Sahalia and Jacod, 2020). For this reason we advocate that noise is an additional *ad hoc*⁷ modelling assumption that is used to reconcile the discrepancy between tick data and macroscopic models when “down-scaling” from macroscopic to microscopic (Aït-Sahalia and Jacod, 2020).

Finding a more appropriate representation for tick data is particularly important when it comes to the investigation of the Epps effect. This is because the decay in correlation is an anomaly that requires a correction under the noise representation. Under the discrete event perspective it is an emergent property resulting from the observer imposing an observation scale. The goal of the noise representation is to try recover the constant underlying induced correlation that is independent of Δt under the presence of *ad hoc* noise.

⁷Popper (1974), pp. 986, “I call a conjecture “ad hoc” if it is introduced [...] to explain a particular difficulty, but if [...] it cannot be tested independently”; here it may be best to think about the noise assumption as “unwarranted” (Hunt, 2012).

On the other hand, the decay in correlation is a fundamental property under the representation of discrete connected events. The ambition here is then to only correct for statistical effects leading to a decay in correlations so that we can recover the theoretical underlying correlation that does depend on Δt .

The key point we are making is that additional *ad hoc* model complexity is required in order to recover the observed phenomena from models which are based on Brownian motions. This type of model complexity is not required using the Hawkes representation. Therefore, based on the principle of parsimony, *i.e.* Occam’s razor, we argue that that the Hawkes representation is the more appropriate representation.

7. Empirical Investigation

We compare the correction methods and detect the underlying processes using banking equities from the Johannesburg Stock Exchange (JSE) with TAQ data for 40 trading days starting from 2019/05/02 to 2019/06/28. The data is extracted from Bloomberg Pro and is processed so that trades with the same time stamp are aggregated using a volume weighted average. The equities considered are: FirstRand Limited (FSR), Absa Group Ltd (ABG), Nedbank Group Ltd (NED) and Standard Bank Group Ltd (SBK).

The correlations are measured for each trading day and the ensemble is reported. The error ribbons are computed such that they contain 95% of the estimates at each Δt between the trading days. They are computed using the Student t -distribution with 39 degrees of freedom and the standard deviation of the estimates between the days at each Δt . Additionally, $t = 0$ starts once the equity pair has each made their first trade and $T = 28,200$ seconds for a seven hour and 50 minute trading day.

We only have one set of observables from empirical TAQ data which means that the second experiment is not well suited for discriminating empirical data. Nonetheless we attempt to apply the experiment because it does reveal something interesting. In order to apply the second experiment we try to re-

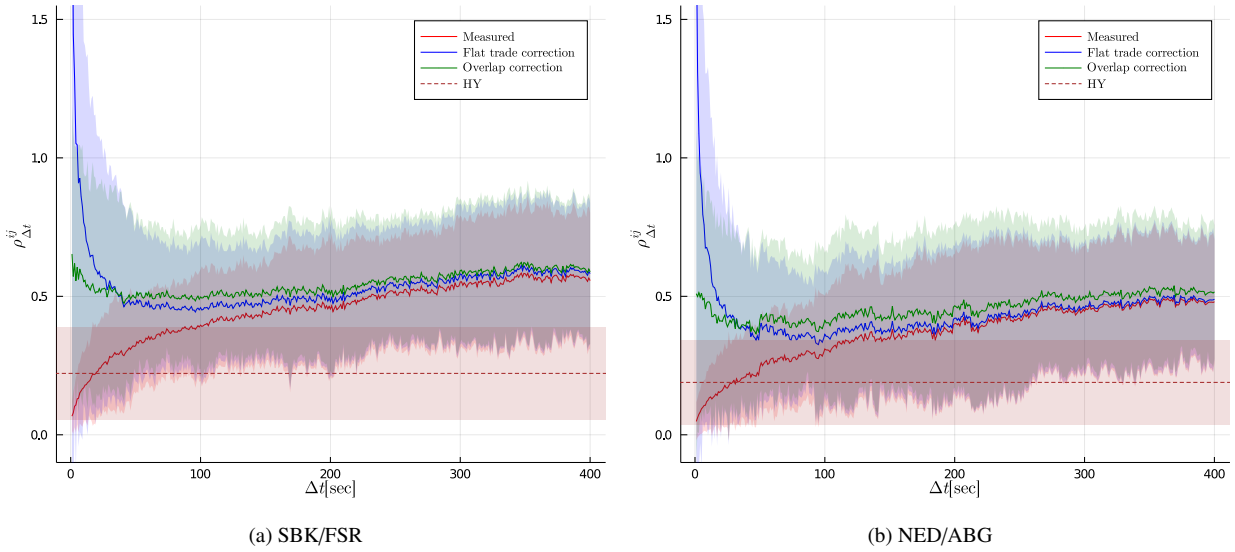


Figure 10: The corrections are applied and compared for the equity pairs (a) SBK/FSR, and (b) NED/ABG. The red line is the measured correlation from the synchronised process (6), the blue line is the flat trade correction (9) and the green line is the overlap correction (7). Lastly the horizontal dashed line is the Hayashi–Yoshida estimator (12).

Table 1: The table reports the mean inter-arrival estimate and the associated standard deviation for the four banking equities over the 40 day trading period.

| Tickers | $1/\hat{\lambda}$ [sec] | $\hat{\sigma}(1/\lambda)$ |
|---------|-------------------------|---------------------------|
| FSR | 12.09 | 19.53 |
| SBK | 13.06 | 21.51 |
| NED | 15.39 | 25.14 |
| ABG | 15.68 | 26.27 |

create the simulation setting by finding equity pairs with similar correlation levels but different average inter-arrivals. Table 1 gives the estimate for the mean and standard deviation for the inter-arrival time over the 40 trading day period. It is clear that the pair FSR and SBK (NED and ABG) have comparable and on average smaller (larger) inter-arrival times respectively. Therefore we will compare the corrections on FSR/SBK against NED/ABG to determine if there is a difference in the decay of the residual Epps effect following the spirit of the second experiment.

Figure 10 compares the correction methods on the pair (a) FSR/SBK and (b) NED/ABG to investigate the residual Epps effect. We see that the variability of the correlation estimates between days is very high but largely remains positive. This is why we chose the banking equities since they have a strong correlation. If the equities are less correlated, the Epps curves can jump between negative and positive between the days. The flat trade correction again over-compensates the correction. The Hayashi–Yoshida estimates do not recover the same estimates as the overlap correction or the saturation level. This is an indication that empirical TAQ data cannot be modelled using Brownian motions alone.

Figure 11 takes a closer look at the overlap correction and the measured correlation for the equity pairs SBK/FSR and

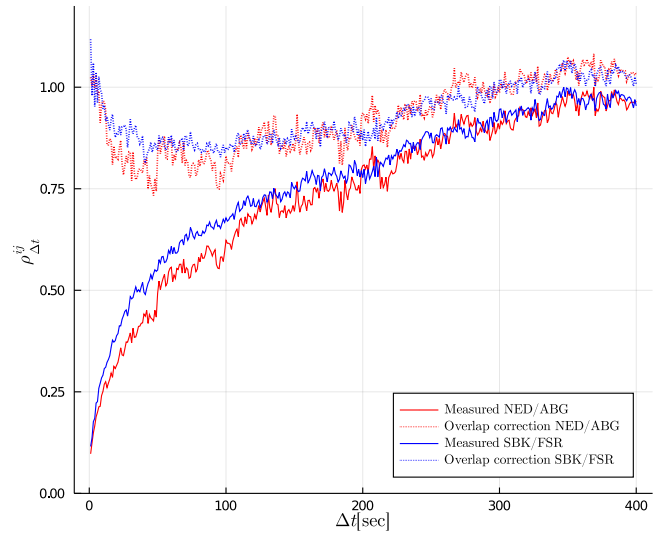


Figure 11: Comparison of the overlap correction (dotted lines) and the measured correlation (solid lines). All the estimates are scaled by the saturation correlation so that clearer comparisons can be made for the equity pairs NED/ABG (red) and SBK/FSR (blue).

NED/ABG investigated in figure 10. Here we re-scale the estimates by the saturation level for better comparison since we have two different equity pairs. We see the measured and correction are similar for both the equity pairs. The similarity of the overlap correction may be due to the fact that the average inter-arrivals are not significantly different. What is more interesting is this U-shaped residual Epps curve which has not been reported in the broader literature. This might be because the corrections are usually not applied at such a fine resolution. Here when $\Delta t > 100$ seconds the decay is present, the

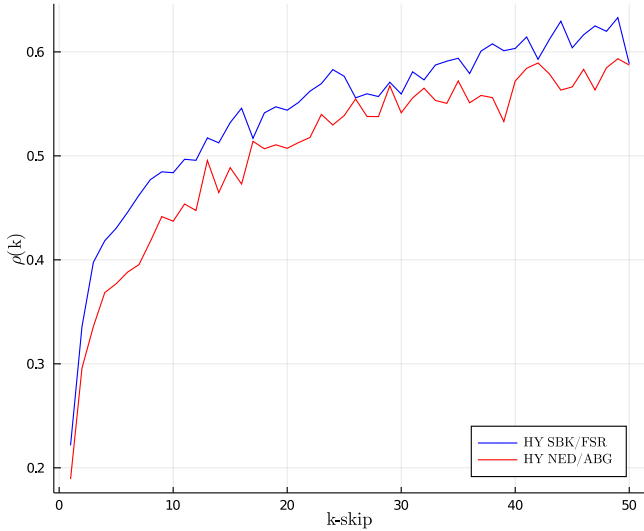


Figure 12: The k -skip sampling with the Hayashi–Yoshida estimator applied to the equity pairs SBK/FSR (blue line) and NED/ABG (red line). The empirical reality suggests the underlying system is from discrete connected events.

decay starts to flatten out for Δt between 50 and 100 seconds, and below 50 seconds the residual correlation starts to rise back towards the saturation level. This behaviour could not be replicated in the simulations with the models and sampling methods considered.

We apply the k -skip Hayashi–Yoshida to better discriminate the underlying process. Figure 12 computes the Hayashi–Yoshida estimates with the k -skip sampling for k ranging from 1 to 50 on the equity pairs SBK/FSR and NED/ABG. Both equity pairs present a decaying correlation for smaller k . This is strong evidence suggesting that empirical TAQ data cannot simply be modelled using a pure diffusion-based process. Additional model complexity such as market microstructure noise or a more appropriate representation using discrete connected events is required.

Even though the evidence in figure 12 may seem convincing, we have yet to control for the effect of lead-lag. Additional work is required to design experiments that incorporate the impact of lead-lags when discriminating the underlying process. This extension may possibly provide insight into this U-shaped residual Epps curve.

8. Conclusion

We derive the Epps effect arising from asynchrony and provide a refined method based on existing work (Münnix et al., 2010, 2011) to correct for this effect. This has been informed by the rich prior literature (Bacry et al., 2013a,b; Mastromatteo et al., 2011; Tóth and Kertész, 2007, 2009; Precup and Iori, 2007). The refinement is simpler to compute as it separates the estimation of correlation from the correction factor without making strong assumptions about the distributional properties of the sampling processes.

The method is compared against the Hayashi–Yoshida estimator (Hayashi and Yoshida, 2005) and a correction using the probability of flat trading (Buccheri et al., 2019) on three models. We found that our correction recovers similar estimates to the Hayashi–Yoshida estimator and outperforms the flat trade correction.

We design three experiments to discriminate the underlying process between diffusion-based processes against diffusion-based processes with *ad hoc* noise, and a process made from discrete connected events. The first two experiments are better suited for simulation scenarios because they repeatedly re-sample the process. The third experiment uses k -skip sampling and allows us to detect the underlying process with one set of observables.

These experiments demonstrate that discrimination is in principle possible but highlights the complexity relating to discriminating between diffusion-based process with *ad hoc* noise against discrete connected events. This is because the two processes recover similar correlation dynamics albeit for very different reasons. We argue that the Hawkes representation is the more appropriate representation because it is the simpler model that recovers the observed phenomenology without *ad hoc* assumptions.

The experiments are applied to trade and quote data from the Johannesburg Stock Exchange. We found an interesting U-shaped residual Epps curve which could not be replicated under simulation. We find evidence using the k -skip sampling suggesting that diffusion-based process alone are insufficient to model empirical trade and quote data. The modelling should be done using discrete connected events or the diffusion process needs to be contaminated with *ad hoc* noise.

More research is required to discriminate between diffusion-based processes with *ad hoc* noise and discrete connected events. Such research may entail designing better experiments to accommodate alternative estimators for discrimination. Moreover, to definitively discriminate on trade and quote data, future experiments must incorporate the effect of lead-lag when discriminating.

If the Epps effect is not just a statistical anomaly that requires a correction then this would mean that we need to be more careful when considering the impact of time scales in decision making if the decisions are predicated on estimates of correlation matrices. In particular, investigating the financial implications and finding the optimal scale(s) to estimate correlation matrices for different types of financial decisions will be a useful exercise.

If tick-by-tick models such as the Hawkes processes are appropriate representations then a reconciliation of time-series properties across various time scales is necessary. Nearly unstable Hawkes processes studied by Jaisson and Rosenbaum (2015, 2016) can be seen as the first steps towards a unified model that fits both microstructure stylised facts and diffusive stylised facts (Bacry et al., 2015) while recovering rough volatility (Gatheral et al., 2018) and hence aspects of long-memory—all from the perspective of the fundamental nature of discrete data generating processes.

Acknowledgements

The authors would like to thank colleagues and others in the community for constructive feedback. P.C. would like to acknowledge the support by the Manuel & Luby Washkansky Scholarship and the South African Statistical Association [grant number 127931].

References

- Ait-Sahalia, Y., Fan, J., Xiu, D., 2010. High-Frequency Covariance Estimates With Noisy and Asynchronous Financial Data. *Journal of the American Statistical Association* 105, 1504–1517. doi:[10.1198/jasa.2010.tm10163](https://doi.org/10.1198/jasa.2010.tm10163).
- Ait-Sahalia, Y., Jacod, J., 2020. From tick data to semimartingales. *The Annals of Applied Probability* 30, 2740–2768. doi:[10.1214/20-AAP1571](https://doi.org/10.1214/20-AAP1571).
- Ait-Sahalia, Y., Mykland, P.A., Zhang, L., 2005. How Often to Sample a Continuous-Time Process in the Presence of Market Microstructure Noise. *The Review of Financial Studies* 18, 351–416. doi:[10.1093/rfs/hhi016](https://doi.org/10.1093/rfs/hhi016).
- Ait-Sahalia, Y., Mykland, P.A., Zhang, L., 2011. Ultra high frequency volatility estimation with dependent microstructure noise. *Journal of Econometrics* 160, 160–175. doi:<https://doi.org/10.1016/j.jeconom.2010.03.028>. realized Volatility.
- Bacry, E., Delattre, S., Hoffmann, M., Muzy, J.F., 2013a. Modelling microstructure noise with mutually exciting point processes. *Quantitative Finance* 13, 65–77. doi:[10.1080/14697688.2011.647054](https://doi.org/10.1080/14697688.2011.647054).
- Bacry, E., Delattre, S., Hoffmann, M., Muzy, J.F., 2013b. Some limit theorems for Hawkes processes and application to financial statistics. *Stochastic Processes and their Applications* 123.
- Bacry, E., Mastromatteo, I., Muzy, J.F., 2015. Hawkes processes in finance. *Market Microstructure and Liquidity* 01, 1550005. doi:[10.1142/S2382626615500057](https://doi.org/10.1142/S2382626615500057).
- Barndorff-Nielsen, O.E., Hansen, P.R., Lunde, A., Shephard, N., 2011. Multivariate realised kernels: Consistent positive semi-definite estimators of the covariation of equity prices with noise and non-synchronous trading. *Journal of Econometrics* 162, 149–169. doi:<https://doi.org/10.1016/j.jeconom.2010.07.009>.
- Buccheri, G., Corsi, F., Peluso, S., 2020. High-Frequency Lead-Lag Effects and Cross-Asset Linkages: A Multi-Asset Lagged Adjustment Model. *Journal of Business & Economic Statistics* 0, 1–22. doi:[10.1080/07350015.2019.1697699](https://doi.org/10.1080/07350015.2019.1697699).
- Buccheri, G., Livieri, G., Pirino, D., Pollastri, A., 2019. A closed-form formula characterization of the Epps effect. *Quantitative Finance* 20, 243–254. doi:[10.1080/14697688.2019.1659992](https://doi.org/10.1080/14697688.2019.1659992).
- Chang, P., Pienaar, E., Gebbie, T., 2020. Malliavin–Mancino Estimators Implemented with Nonuniform Fast Fourier Transforms. *SIAM Journal on Scientific Computing* 42, B1378–B1403. doi:[10.1137/20M1325903](https://doi.org/10.1137/20M1325903).
- Chang, P., Pienaar, E., Gebbie, T., 2021. The Epps effect under alternative sampling schemes. *Physica A: Statistical Mechanics and its Applications* 583, 126329. doi:<https://doi.org/10.1016/j.physa.2021.126329>.
- Corsi, F., Peluso, S., Audrino, F., 2015. Missing in Asynchronicity: A Kalman-EM Approach for Multivariate Realized Covariance Estimation. *Journal of Applied Econometrics* 30, 377–397. doi:<https://doi.org/10.1002/jae.2378>.
- Epps, T.W., 1979. Comovements in stock prices in the very short run. *Journal of the American Statistical Association* 74, 291–298.
- Gatheral, J., Jaisson, T., Rosenbaum, M., 2018. Volatility is rough. *Quantitative Finance* 18, 933–949. doi:[10.1080/14697688.2017.1393551](https://doi.org/10.1080/14697688.2017.1393551).
- Griffin, J.E., Oomen, R.C., 2011. Covariance measurement in the presence of non-synchronous trading and market microstructure noise. *Journal of Econometrics* 160, 58–68.
- Hawkes, A.G., 1971. Spectra of some self-exciting and mutually exciting point processes. *Biometrika* 58, 83–90.
- Hawkes, A.G., 2018. Hawkes processes and their applications to finance: a review. *Quantitative Finance* 18, 193–198. doi:[10.1080/14697688.2017.1403131](https://doi.org/10.1080/14697688.2017.1403131).
- Hayashi, T., Yoshida, N., 2005. On covariance estimation of non-synchronously observed diffusion processes. *Bernoulli* 11, 359–379. doi:[10.3150/bj/1116340299](https://doi.org/10.3150/bj/1116340299).
- Hendricks, D., Gebbie, T., Wilcox, D., 2016. Detecting intraday financial market states using temporal clustering. *Quantitative Finance* 16, 1657–1678. doi:[10.1080/14697688.2016.1171378](https://doi.org/10.1080/14697688.2016.1171378).
- Hunt, J.C., 2012. On ad hoc hypotheses*. *Philosophy of Science* 79, 1–14.
- Jaisson, T., Rosenbaum, M., 2015. Limit theorems for nearly unstable Hawkes processes. *The Annals of Applied Probability* 25, 600–631. doi:[10.1214/14-aap1005](https://doi.org/10.1214/14-aap1005).
- Jaisson, T., Rosenbaum, M., 2016. Rough fractional diffusions as scaling limits of nearly unstable heavy tailed Hawkes processes. *The Annals of Applied Probability* 26, 2860–2882. doi:[10.1214/15-AAP1164](https://doi.org/10.1214/15-AAP1164).
- Malliavin, P., Mancino, M., 2002. Fourier series method for measurement of multivariate volatilities. *Finance and Stochastics* 6, 49–61. doi:[10.1007/s780-002-8400-6](https://doi.org/10.1007/s780-002-8400-6).
- Malliavin, P., Mancino, M., 2009. A Fourier transform method for nonparametric estimation of multivariate volatility. *Ann. Statist.* 37, 1983–2010. doi:[10.1214/08-AOS633](https://doi.org/10.1214/08-AOS633).
- Mastromatteo, I., Marsili, M., Zoi, P., 2011. Financial correlations at ultra-high frequency: theoretical models and empirical estimation. *The European Physical Journal B* 80, 243–253. doi:[10.1140/epjb/e2011-10865-y](https://doi.org/10.1140/epjb/e2011-10865-y).
- Münnix, M.C., Schäfer, R., Guhr, T., 2010. Impact of the tick-size on financial returns and correlations. *Physica A: Statistical Mechanics and its Applications* 389, 4828–4843. doi:<https://doi.org/10.1016/j.physa.2010.06.037>.
- Münnix, M.C., Schäfer, R., Guhr, T., 2011. Statistical causes for the Epps effect in microstructure noise. *International Journal of Theoretical and Applied Finance* 14, 1231–1246. doi:[10.1142/S0219024911006838](https://doi.org/10.1142/S0219024911006838).
- Peluso, S., Corsi, F., Mira, A., 2014. A Bayesian High-Frequency Estimator of the Multivariate Covariance of Noisy and Asynchronous Returns. *Journal of Financial Econometrics* 13, 665–697. doi:[10.1093/jjfinec/mbu017](https://doi.org/10.1093/jjfinec/mbu017).
- Popper, K., 1974. Replies to my critics, in: Schilpp, P.A. (Ed.), *The Philosophy of Karl Popper*. Open Court, pp. 961–1197.
- Precup, O.V., Iori, G., 2007. Cross-correlation measures in the high-frequency domain. *The European Journal of Finance* 13, 319–331. doi:[10.1080/13518470600813565](https://doi.org/10.1080/13518470600813565).
- Renò, R., 2003. A closer look at the Epps effect. *International Journal of Theoretical and Applied Finance* 06, 87–102. doi:[10.2139/ssrn.314723](https://doi.org/10.2139/ssrn.314723).
- Toke, I., Pomponio, F., 2012. Modelling Trades-Through in a Limit Order Book Using Hawkes Processes. *Economics: The Open-Access, Open-Assessment E-Journal* 6, 1–23. doi:[10.2139/ssrn.1973856](https://doi.org/10.2139/ssrn.1973856).
- Tóth, B., Kertész, J., 2007. Modeling the Epps effect of cross correlations in asset prices, in: Kertész, J., Bornholdt, S., Mantegna, R.N. (Eds.), *Noise and Stochastics in Complex Systems and Finance*, International Society for Optics and Photonics. SPIE, pp. 89–97. URL: <https://doi.org/10.1117/12.727127>, doi:[10.1117/12.727127](https://doi.org/10.1117/12.727127).
- Tóth, B., Kertész, J., 2009. The Epps effect revisited. *Quantitative Finance* 9, 793–802. doi:[10.1080/14697680802595668](https://doi.org/10.1080/14697680802595668).
- Zhang, L., 2010. Estimating covariation: Epps effect, microstructure noise. *Journal of Econometrics* 160, 33–47. doi:[10.1016/j.jeconom.2010.03.012](https://doi.org/10.1016/j.jeconom.2010.03.012).
- Zhang, L., Mykland, P.A., Ait-Sahalia, Y., 2005. A tale of two time scales: Determining integrated volatility with noisy high-frequency data. *Journal of the American Statistical Association* 100, 1394–1411.

Appendix A. Estimators for market microstructure noise

We apply two alternative estimators in order to try and discriminate between the MMN and Hawkes price model. The two estimators considered here are the Quasi-Maximum Likelihood Estimator (QMLE) from Ait-Sahalia et al. (2010) and the Kalman-EM (KEM) estimator from Corsi et al. (2015) which is a special case of the Multi-asset Lagged Adjustment (MLA) estimator from Buccheri et al. (2020).⁸

The QMLE and KEM estimator addresses both asynchrony and market microstructure noise. However, the way the two

⁸We do not use the MLA estimator here because we found that the estimator overestimates the correlation in our models which have no lead-lag dependencies by trying to account for lead-lags.

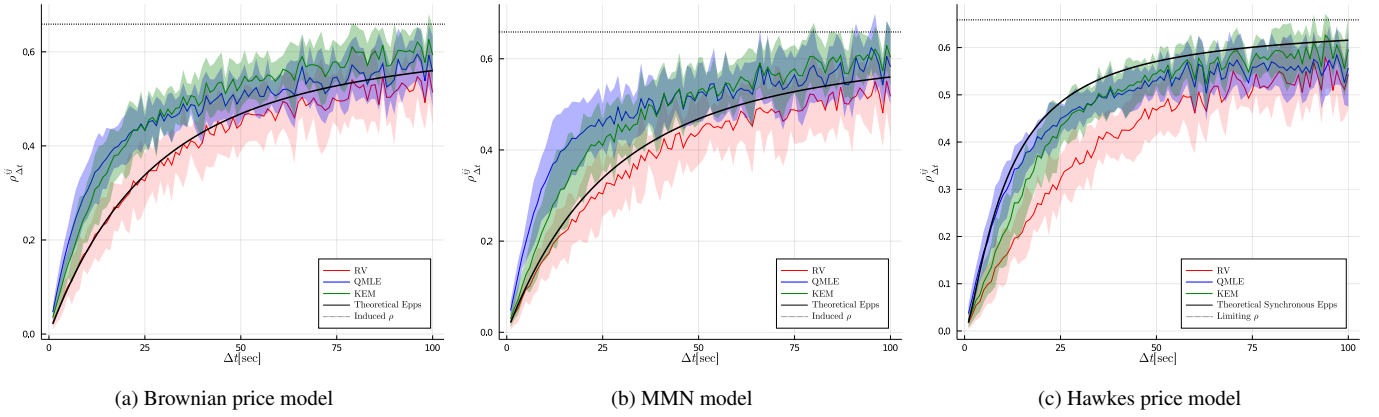


Figure A.13: The measured correlation (red line), QMLE (blue line) and KEM estimate (green line) are compared on (a) the Brownian price model, (b) the MMN model and (c) the Hawkes price model using Poisson sampling.

estimators address asynchrony does not fit easily within our experimental framework.

First, the QMLE addresses asynchrony by applying a different sampling approach called the generalised sampling time. We use the most naive version of the sampling scheme that reduces to previous tick interpolation so that the estimator can fit within our experimental framework.

Second, the KEM addresses asynchrony by using the Kalman filter based smoother to access the latent states. The caveat here is that the observations and missing observations must all occur on a homogeneous grid. This is problematic within our experimental framework because we apply Poisson and Hawkes sampling to obtain the observables instead of a Bernoulli censoring approach. Even though Poisson sampling and independent Bernoulli censoring are equivalent, the subtle difference is that observables from Poisson sampling do not necessarily lie on a homogeneous grid. This creates an ambiguity when creating a homogeneous grid at different time scales Δt . For small Δt , if an observable is near two grid points, a decision needs to be made in terms of which grid point the observable should be shifted to. For large Δt , if there are more than two observables near the same grid point, a decision needs to be made in terms of which observable should be on that grid point. To overcome these issues, we simply apply previous tick interpolation and create a synchronised grid to feed into the KEM estimator. This also ensures that the estimator fits within our experimental framework.

We reduce the simulation size to T being 6.5 hours (23,400 seconds) and we only perform 10 replications for this proof of concept. The reason for this is because of the long compute time of the QMLE which requires the optimisation of four likelihoods to obtain a correlation estimate. Otherwise the parameter settings for the models and the experimental setup remain the same as before.

Figure A.13 compares the measured correlation, QMLE and KEM estimates for the (a) the Brownian price model, (b) the MMN model and (c) the Hawkes price model under Poisson sampling. We see that the QMLE and KEM estimates are larger than that of the measured correlation for all three models. This

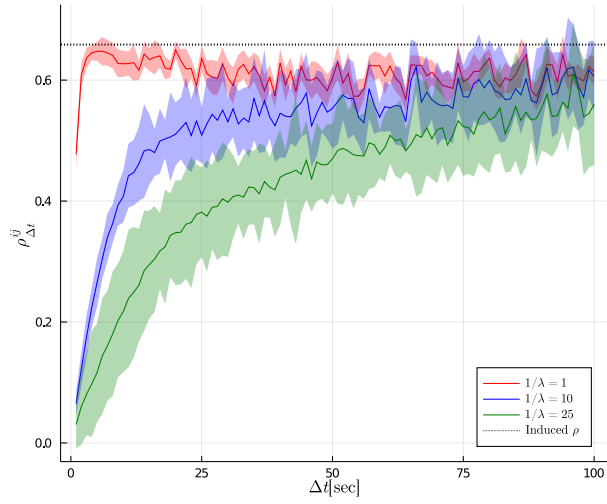
larger estimate is a result of the QMLE and KEM adjusting for market microstructure noise which may or may not be present depending on the model.

We perform experiment 2 from section 5 using the two estimators to see if they can help us discriminate between the MMN and the Hawkes price model. This can be seen in figure A.14. We see that both processes lead to similar behaviours in the residual Epps effect. The case when $1/\lambda = 1$ is notable as these arguably present different behaviours between the two models. However the difference is not as clear cut as in the case of a simple Brownian motion against these two processes. Therefore it does not seem like discrimination between the two processes is possible with our current experiments.

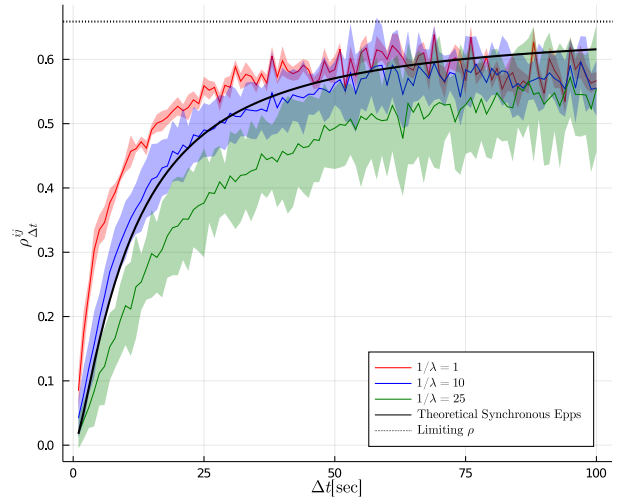
What is interesting about figure A.14 is that the behaviour of the residual Epps effect under different sampling frequencies (from the observables) are the reversal of what is seen in figure 8. We see that there is a larger (smaller) decay in the residual Epps effect for larger (smaller) $1/\lambda$. We argue that this is a result of the interplay between the estimators correcting for noise and the signal-to-noise ratio from the different time scales induced by the observables. The estimators pick up a larger signal-to-noise ratio which leads to a larger correction when $1/\lambda$ is small, and the estimators pick up a smaller signal-to-noise ratio which leads to a smaller correction when $1/\lambda$ is large.

What is concerning is that the estimators also seem to be correcting for noise in the Hawkes price model. The estimators are misconstruing the fundamental discreteness in the model as noise. This is because the noise assumption is *a-priori* built into the estimators. Addressing this *a-priori* assumption should be considered when picking estimators and designing experiments to discriminate between the two processes.

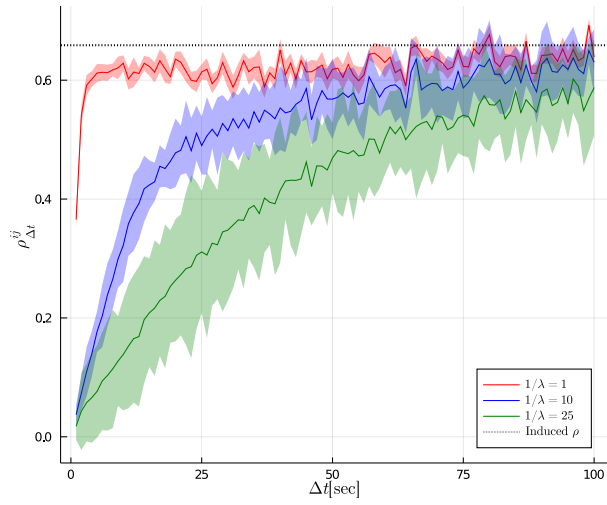
Other estimators that could potentially help us discriminate between the MMN and the Hawkes price model include the estimators from Barndorff-Nielsen et al. (2011); Peluso et al. (2014) and Münnix et al. (2011). Additionally, the MLA estimator from Buccheri et al. (2020) could prove useful when trying to discriminate under the presence of lead-lag.



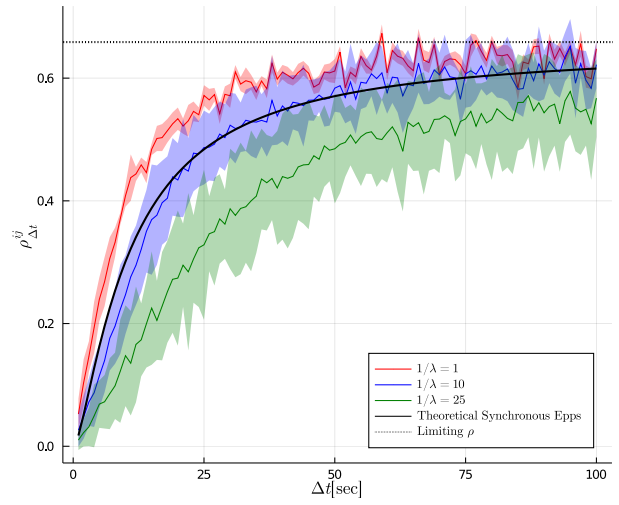
(a) QMLE on MMN model



(b) QMLE on Hawkes price model



(c) KEM on MMN model



(d) KEM on Hawkes price model

Figure A.14: The QMLE (first row) and KEM (second row) applied on the MMN (first column) and the Hawkes price model (second column) for three sampling frequencies of observables. The three sampling frequencies chosen are: $1/\lambda = 1, 10, 25$ which corresponds to the red, blue, green lines respectively. The thick line is the theoretical synchronous Epps effect given by (15) and the horizontal dotted line is the induced/limiting ρ set to be approximately 0.65 as before.